Electrophoretic Mobility Shift Assay—The electrophoretic mobility shift assay (EMSA) for the GC box and CRE was performed as described previously (24). Briefly, oligonucleotides were labeled with [γ-^{32}P]ATP using T4 polynucleotide kinase and then annealed to double-strand oligonucleotides. Specific oligonucleotides for the GC box and CRE were prepared according to the nucleotide sequences of the rat *PP2Ac*α promoter region. Oligonucleotides used are as follows: GC box (−155), 5′-CGGGAGGACCACGCCCCAAAAGCGAAGC-3′; GC box (−155)-Mt, 5′-CGGGAGGACCACAACCCAAAAGCGAAGC-3′; CRE (−26), 5′-GACGCCGGCCTGACGTCACCACGCC-3′; CRE (−26)-Mt, 5′-GACGCCGGCCTGTGGTCACCACGCC -3′. Binding reactions were carried out in 15 μl of reaction mixture (25 mM Tris, pH 7.0, 6.25 mM $MgCl_2$, 0.5 mM EDTA, 0.5 mM dithiothreitol, 50 mM KCl, and 10% glycerol) containing 10 μg of nuclear extract, and 25 ng of labeled oligonucleotide. For the supershift assay, specific antibodies were added to the reaction mixture during the 30-min binding reaction.

Indirect Immunofluorescence Microscopy—After treatment with 5 μM thapsigargin or 10 μM BAPTA-AM for 2 h, cells incubated on Lab-Tek chamber slides (Nunc) were fixed with 3% paraformaldehyde for 20 min at room temperature and washed three times with PBS. Cells were permeabilized in 1% Triton X-100 in PBS for 10 min and washed three times with PBS. They were blocked with 1% bovine serum albumin in PBS for 30 min at room temperature, washed three times with PBS, and then incubated with antiphospho-CREB (Ser-133) overnight at 4 °C. Cells were washed with PBS four times and incubated with FITC-labeled anti-rabbit IgG antibody for 30 min in a dark room. The immunoreactive signals were visualized by indirect immunofluorescence microscopy.

RESULTS

Elevation of $[Ca^{2+}]_i$ Gradually Accelerates Cell Damage and Apoptosis in H9c2 Cells—To modify the level of $[Ca^{2+}]_i$ in H9c2 cells, the cells were treated with 5 μM thapsigargin (25), an inhibitor for sarcoplasmic/endoplasmic reticulum Ca^{2+} ATPase to increase $[Ca^{2+}]_i$, or with 10 μM BAPTA-AM (26), a cell permeable Ca^{2+} chelator to decrease $[Ca^{2+}]_i$, for 0–4 h. As shown in Fig. 1*A*, with thapsigargin, $[Ca^{2+}]_i$ shows a transient increase within the first 10 min. It then decreases to the basal level till 30 min, but again increases and retains elevated until 120 min, before gradually decreasing to the initial level. In contrast, with BAPTA-AM, $[Ca^{2+}]_i$ shows a continuous lowering during the treatment. To investigate the influence of the long term change of $[Ca^{2+}]_i$ on susceptibility to oxidative stress-induced cell injury, cells were treated with Ca^{2+} modulators (*i.e.* thapsigargin and BAPTA-AM) for 4 h then exposed to 75 μM hydrogen peroxide (H_2O_2) for 0–120 min, and cell damage was examined at predetermined times using the LDH release assay as described in the methods. In Fig. 1*B*, the release of LDH by H_2O_2 was observed only at 120 min in the medium of untreated cells. However, the release by H_2O_2 was initially observed at 60 min and increased at 120 min in the cells treated with thapsigargin. In contrast, BAPTA-AM treatment completely suppressed the release of LDH by H_2O_2 throughout the 120 min. Next, to investigate whether apoptosis is involved in the mechanism of thapsigargin-induced cell damage, cells were treated with Ca^{2+} modulators for 4 h then exposed to H_2O_2 (75 μM) for 2 h, and apoptosis was examined. Fig. 1*C* shows that TUNEL-positive fluorescence intensity was increased slightly by H_2O_2 (*upper*), but was significantly enhanced after the pretreatment with thapsigargin (*middle*). In contrast, no change was observed in the fluorescent intensity of the BAPTA-AM-treated cells with or without H_2O_2 (*lower*). Collectively, these results indicate that the susceptibility to apoptosis was enhanced with a long term elevation of $[Ca^{2+}]_i$, but was suppressed with the lowering of $[Ca^{2+}]_i$ in the cells under oxidative stress with H_2O_2, suggesting that the continuous change of $[Ca^{2+}]_i$ influences the susceptibility to apoptosis.

The Long Term Change of $[Ca^{2+}]_i$ Influences Akt Signaling in H9c2 Cells—To know the role of $[Ca^{2+}]_i$ in cell survival signaling, we focused on the effect of Ca^{2+} modulators on Akt signaling. Previously, we found that the Akt signaling pathway is responsible for the cytoprotective mechanism in H9c2 cells under conditions of stress such as serum starvation with retinoic acid (16), and oxidative stress with hydrogen peroxide (27). Although elevations in Ca^{2+} act as a signal, a prolonged increase in the concentration of Ca^{2+} can be lethal (1). Moreover, cell signaling molecules including transcription factors are activated differentially by the amplitude and duration of the response to Ca^{2+} (28). In the present study, H9c2 cells were treated with Ca^{2+} modulators such as thapsigargin (5 μM) and BAPTA-AM (10 μM) for over 2 h to induce a long term change of $[Ca^{2+}]_i$. After the treatments, the phosphorylation levels of Ser-473 and Thr-308 of Akt were examined. The phosphorylation of Thr-308 located in the kinase catalytic domain of Akt is necessary for the activation, and the phosphorylation of Ser-473 located in the regulatory domain of Akt supports the activation. As shown in Fig. 2, *A* (*right*) and *B*, the treatment with BAPTA-AM increased the phosphorylation of Akt both at Ser-473 and Thr-308, and the phosphorylation level increased to a maximum at 2 h, and was sustained thereafter till 4 h. In contrast, the phosphorylation of Akt decreased in a time-dependent manner with thapsigargin (Fig. 2, *A* (*left*) and *B*). Next we examined whether Ca^{2+} modulators also have an effect on the kinase activity of Akt. Fig. 2*C* shows that Akt activity is suppressed after the treatment with thapsigargin, but increased with BAPTA-AM. These results were consistent with the change in the phosphorylation status of Akt on treatment with Ca^{2+} modulators such as thapsigargin and BAPTA-AM. Together, Akt signaling was suppressed by the long term elevation of $[Ca^{2+}]_i$ with thapsigargin, but was enhanced by the long term lowering of $[Ca^{2+}]_i$ with BAPTA-AM. This suggests a Ca^{2+}-dependent regulation of Akt signaling in H9c2 cells. Furthermore, the Ca^{2+}-induced suppression of Akt signaling was compatible with the enhanced susceptibility to apoptosis in H9c2 cells treated with H_2O_2 (Fig. 1, *B* and *C*).

The Expression of PP2Acα *Is Transcriptionally Regulated by Ca^{2+} Modulators*—3-Phosphoinositide-dependent protein kinase (PDK1) is known to be responsible for phosphorylating Akt at Thr-308, and is activated by both phosphatidylinositol (3,4,5)-trisphosphate and phosphatidylinositol (3,4,)-bisphosphate, products of PI3K (9, 10). To investigate whether the upstream kinases are involved in the regulation of Akt by the change of $[Ca^{2+}]_i$, the activities for PI3K and PDK1 were measured in the cells treated with Ca^{2+} modulators. However, neither activities showed any significant change even if the cells were treated with thapsigargin or BAPTA-AM for 0–4 h (data not shown). Therefore, we focused on Ser/Thr protein phosphatases that could dephosphorylate and inactivate Akt to regulate the Akt signaling pathway (7). To investigate whether $[Ca^{2+}]_i$ levels affect the expression of protein Ser/Thr phosphatases, the cells were treated with 5 μM thapsigargin or 10 μM BAPTA-AM for 0–4 h, and transcriptional levels were estimated by Northern blot analysis for protein phosphatase 2A catalytic subunit α (PP2Acα) and protein phosphatase 1α catalytic subunit (PP1αc). In Fig. 3*A*, the level of PP2Acα mRNA was increased by thapsigargin but decreased by BAPTA-AM. In contrast, the mRNA level of PP1αc was not significantly changed by the Ca^{2+} modulators. In the immunoblot analysis, the protein level of PP2Acα was increased by thapsigargin but decreased by BAPTA-AM (Fig. 3*B*). However, the protein level of PP1αc was not influenced by thapsigargin or BAPTA-AM. The protein level of calcineurin/PP2B was not influenced by thapsigargin or BAPTA-AM either (data not shown). These results were consistent with results of the change of transcriptional levels for the phosphatases in the cells treated with each Ca^{2+} modulator. The enzymatic activity

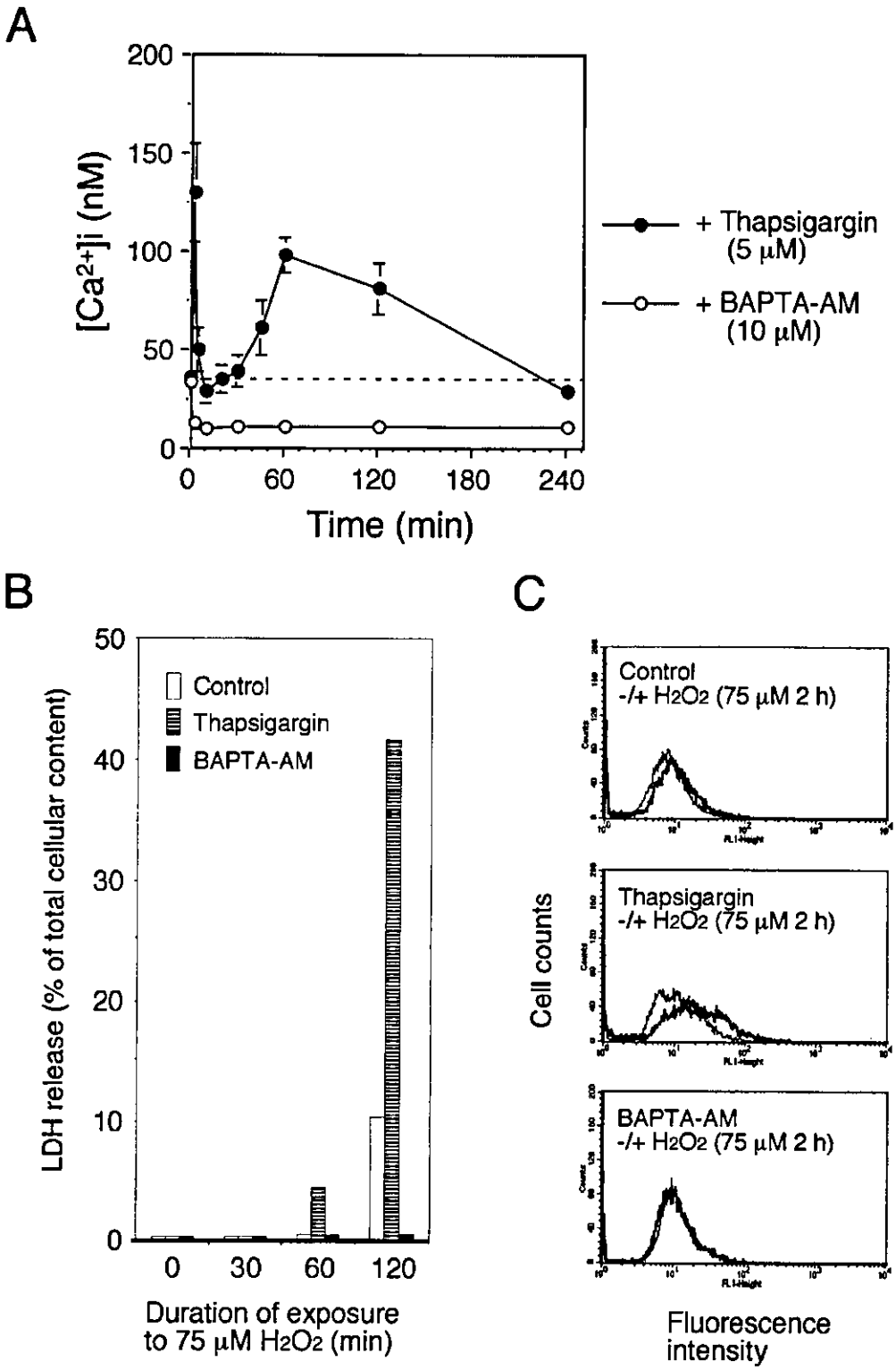

FIG. 1. **The long term elevation of $[Ca^{2+}]_i$ accelerates apoptosis in H9c2 cells under oxidative stress with H_2O_2.** *A*, H9c2 cells were treated with thapsigargin (5 μM) or BAPTA-AM (10 μM) for the periods indicated, and $[Ca^{2+}]_i$ was measured using Fura-2-AM as described under "Materials and Methods." Each value represents the mean ± S.D. of four independent experiments. *B*, after 4 h of treatment with thapsigargin (5 μM) or BAPTA-AM (10 μM) or not, the cells were incubated with H_2O_2 (75 μM) for the periods indicated. Cell injury was estimated by measuring the release of LDH in the culture medium as described under "Materials and Methods." The LDH release is shown as the proportion of total cellular LDH in the medium to total cellular LDH. Each value represents the mean of three experiments, and the S.D. was always within 10% of the mean. *C*, DNA double-stranded breaks were detected by the TUNEL method as described under "Materials and Methods." Cells were treated with either thapsigargin (5 μM) or BAPTA-AM (10 μM) for 4 h and untreated cells were prepared as a control. Then the cells were treated with (*thick lines*) or without (*thin lines*) H_2O_2 (75 μM) for 2 h. The results were reproducible in three independent experiments.

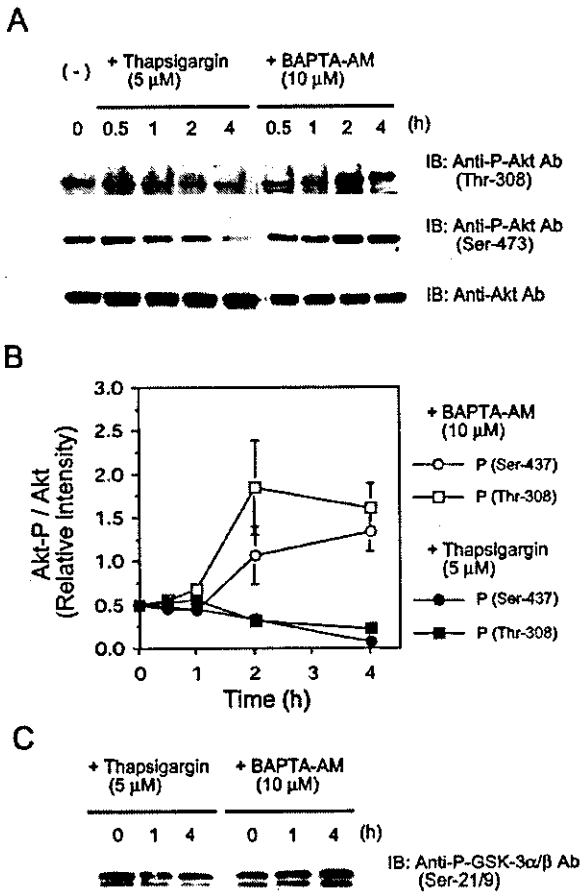

FIG. 2. **Ca^{2+} modulators influence the phosphorylation and kinase activity of Akt in H9c2 cells.** H9c2 cells were cultured in the presence of either thapsigargin (5 μM) or BAPTA-AM (10 μM) for the periods indicated. *A*, Akt phosphorylation was detected in the cell lysates by immunoblot analysis (*IB*) with anti-phospho-Akt (Ser-473), anti-phospho-Akt (Thr-308), and anti-Akt antibodies. *B*, quantitative data for the phosphorylation status of Akt shown in *A*. The band intensity was estimated densitometrically, and the phosphorylation rate is expressed as the relative intensity of the phosphorylated Akt (Akt-P)/Akt. Each value represents the mean ± S.D. of four independent experiments. *C*, Akt kinase activity was assayed as described under "Materials and Methods" using GSK-3α/β as a substrate. Phosphorylated GSK-3α/β (Ser-21/9), the enzymatic products of Akt, was detected by immunoblot analysis using specific antibody. The data represent three independent experiments.

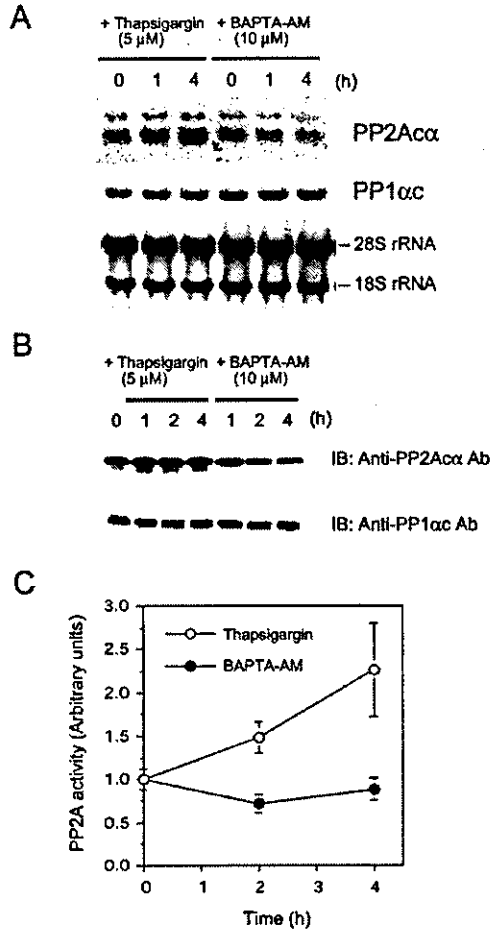

FIG. 3. **The expression and phosphatase activity of PP2Acα are regulated by Ca^{2+} modulators in H9c2 cells.** H9c2 cells were treated with thapsigargin (5 μM) or BAPTA-AM (10 μM) for the periods indicated. *A*, transcriptional levels of PP2Acα and PP1αc were evaluated by Northern blot analysis as described under "Materials and Methods." An EcoRI-PvuII fragment of 680 bp and a PstI-SmaI fragment of 600 bp were prepared from cDNAs for PP2Acα and PP1αc, respectively, and were used as cDNA probes after labeling with [α-^{32}P]dCTP. *B*, protein levels for PP2Acα and PP1cα were estimated by immunoblot analysis using specific antibodies. The data represent three independent experiments. *C*, protein phosphatase activity was assayed photometrically as described under "Materials and Methods." Each value represents the mean ± S.D. of four independent experiments.

of PP2A was also assayed in the cells treated with thapsigargin or BAPTA-AM for 0–4 h. As shown in Fig. 3*C*, the activity of PP2A increased with thapsigargin by ~2-fold compared with that of untreated cells. In contrast, the activity was slightly suppressed after 2 h treatment with BAPTA-AM. Collectively, these results indicate that PP2Acα expression is transcriptionally regulated by the long term change of $[Ca^{2+}]_i$ to control the phosphorylation status of target molecules including Akt.

Inhibition of PP2A Activity by Okadaic Acid Enhanced the Phosphorylation of Akt—Okadaic acid, a polyether toxin from the marine black sponge *Halichondria okadai* is a highly selective inhibitor of PP2A (29). To establish a link between Akt and PP2A, the influence of okadaic acid on Akt signaling was investigated with cells treated with okadaic acid. The cells were treated with okadaic acid (100 nM) for 0–30 min. The phosphorylation level of Akt was estimated by immunoblot analysis using specific antibodies. Akt kinase and PP2A activities were measured as described above. As shown in Fig. 4*A*, okadaic acid reduced the activity of PP2A by ~30%, and increased the phosphorylation level of Akt (both Thr-308 and Ser-473) and Akt kinase activity. Next, we examined whether the decrease in phosphorylation of Akt caused by thapsigargin could be reversed by okadaic acid. The cells were preincubated with thapsigargin (5 μM) for 4 h, and treated with or without okadaic acid (100 nM) for another 30 min, then the phosphorylation level of Akt was examined as described above. As shown in Fig. 4*B*, okadaic acid suppressed PP2A activity, and this reversed the decrease in phosphorylation of Akt with thapsigargin. Okadaic acid enhanced the phosphorylation of Akt at concentrations higher than 50 nM (data not shown). These results indicate that the function of PP2A can regulate the phosphorylation status of Akt in H9c2 cells.

Inhibition of PP2A Activity by Okadaic Acid Suppressed Apoptotic Cell Damage in H9c2 Cells Treated with Thapsigargin and H_2O_2—To establish a link between PP2A and Ca^{2+}-dependent enhancement of apoptosis, the influence of okadaic acid on apoptosis was investigated using cells treated with okadaic acid. In Fig. 5*A*, cells were treated with or without

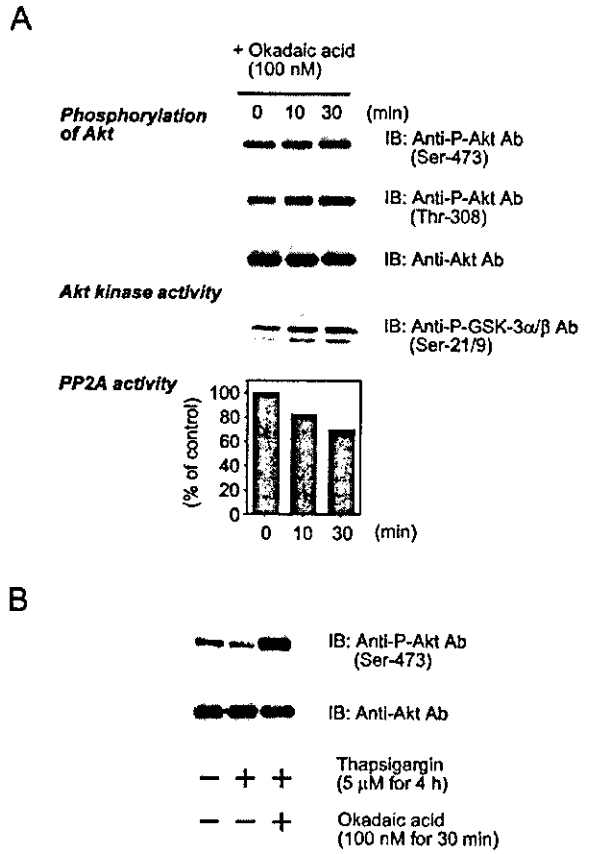

FIG. 4. **Inhibition of PP2A activity by okadaic acid enhances the phosphorylation of Akt in H9c2 cells.** *A*, H9c2 cells were incubated with 100 nM okadaic acid for 0–30 min. The phosphorylation level of Akt was estimated by immunoblot analysis using specific antibodies. The activities for Akt and PP2A were measured as described under "Materials and Methods." The data for PP2A activity represent the mean of three independent experiments. *B*, cells were preincubated with thapsigargin (5 μM) for 4 h then treated with or without okadaic acid (100 nM) for 30 min. The phosphorylation level of Akt (Ser-473) was examined by immunoblot analysis as described above. The data represent three independent experiments.

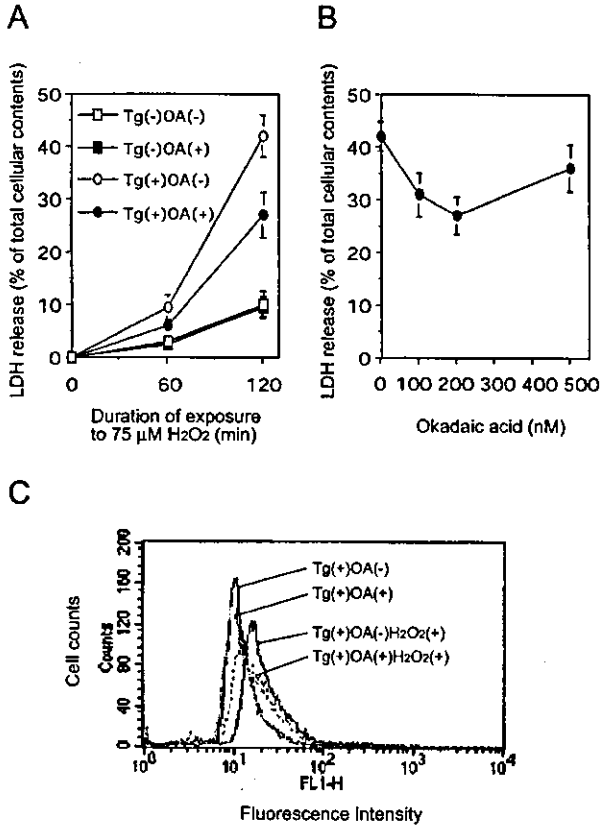

FIG. 5. **Inhibition of PP2A activity by okadaic acid suppresses apoptosis in H9c2 cells treated with thapsigargin and H_2O_2.** *A*, H9c2 cells were preincubated with or without thapsigargin (*Tg*, 5 μM) for 4 h then treated with or without okadaic acid (*OA*, 200 nM) for 30 min. Then the cells were treated with H_2O_2 (75 μM) for the periods indicated. Cell injury was estimated by measuring the release of LDH in the culture medium as described in Fig. 1*B*. Each value represents the mean ± S.D. of four independent experiments. *B*, cells were preincubated with thapsigargin (5 μM) for 4 h then treated with different concentrations of okadaic acid (0–500 nM) for 30 min. Then the cells were incubated with H_2O_2 (75 μM) for the periods indicated. Cell injury was estimated by measuring the release of LDH in the culture medium as described above. Each value represents the mean ± S.D. of four independent experiments. *C*, DNA double-stranded breaks were detected by the TUNEL method as described in Fig. 1*C*. Cells were treated with thapsigargin (5 μM) for 4 h then treated with or without okadaic acid (100 nM). Thereafter, the cells were treated with or without H_2O_2 (75 μM) for 2 h. The results were reproducible in three independent experiments.

thapsigargin (5 μM) for 4 h then treated with okadaic acid (200 nM) for 30 min. Then cells were exposed to H_2O_2 (75 μM) for 0–2 h, and cell damage was examined at predetermined times using LDH release assay. The results showed that treatment with okadaic acid suppressed the Ca^{2+}-dependent enhancement of cell damage in cells treated with thapsigargin and H_2O_2. Fig. 5*B* shows a dose-dependent effect of okadaic acid on the Ca^{2+}-dependent enhancement of cell damage. Cells were treated with thapsigargin (5 μM) for 4 h then treated with different concentrations of okadaic acid (0–500 nM) for 30 min. Thereafter, cells were exposed to H_2O_2 (75 μM) for 2 h, and cell damage was examined using LDH release assay. Okadaic acid showed maximal cytoprotective effects at a limited concentration range around 100–200 nM. The protective effect of okadaic acid was rather diminished at concentrations higher than 500 nM (data not shown). Fig. 5*C* shows the effect of okadaic acid on Ca^{2+}-dependent enhancement of apoptosis. Cells were treated with thapsigargin (5 μM) for 4 h then treated with or without okadaic acid (100 nM) for 30 min. Then cells were exposed to H_2O_2 (75 μM) for 2 h, and apoptosis was examined by the TUNEL method. After thapsigargin treatment without okadaic acid, TUNEL-positive fluorescence intensity was significantly increased by H_2O_2 (Figs. 1*C* and 5*C*, Tg(+)OA(−)H_2O_2(+)). In contrast, okadaic acid reduced the TUNEL-positive fluorescence intensity even in the cells treated with thapsigargin and H_2O_2 (Fig. 5*C*, Tg(+)OA(+)H_2O_2(+)) compared with that of cells treated with thapsigargin and H_2O_2 without okadaic acid. Okadaic acid did not solely affect the fluorescence intensity in cells with thapsigargin without H_2O_2 (Fig. 5*C*, Tg(+)OA(−) and Tg(+)OA(+)). However, it is noteworthy that okadaic acid shows an antiapoptotic effect at a limited concentration range around 100 nM. At concentrations above 500 nM, the antiapoptotic effect of okadaic acid was diminished or rather it showed enhancement of apoptosis in the cells treated with thapsigargin and H_2O_2 (data not shown). This may be explained by the dualistic effect of inhibiting the effects of PP1 and PP2A on both apoptosis and cell proliferation in cells exposed to okadaic acid or microcystin-LR (30). Together, these results indicate that okadaic acid, a specific inhibitor of PP2A, inhibits apoptotic cell damage in H9c2 cells treated with thapsigargin and H_2O_2, and strongly suggests that PP2A up-regulates the Ca^{2+}-dependent enhancement of apoptosis by dephosphorylating Akt to inhibit cell survival signaling.

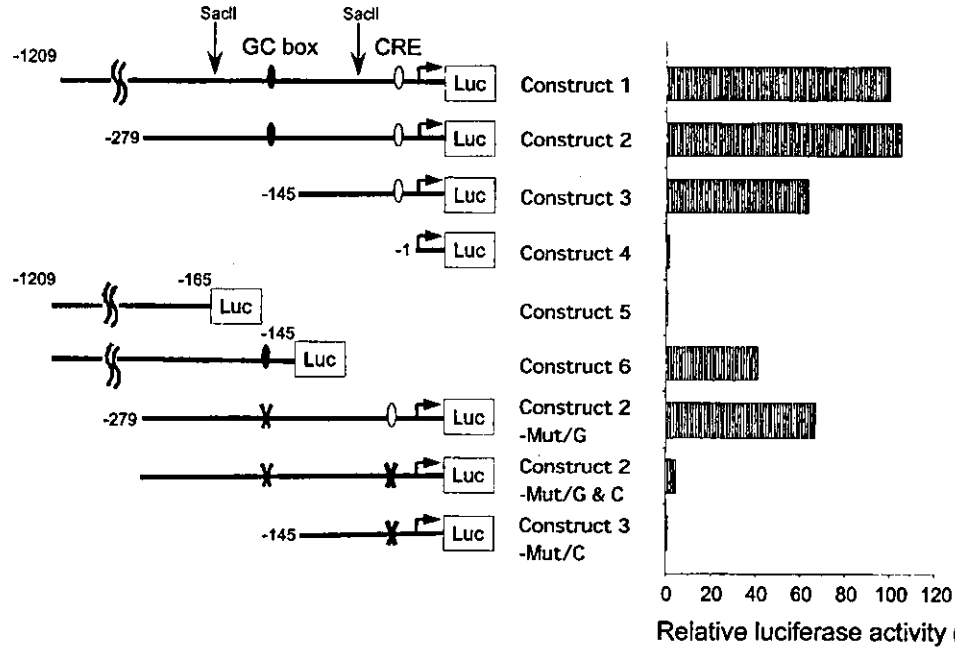

FIG. 6. **Both the GC box and CRE are important for basal activity of the PP2Acα promoter in H9c2 cells.** *Left*, schematic representation of luciferase vector constructs for the rat PP2Acα promoter. Each luciferase vector construct was generated as described under "Materials and Methods." A putative GC box site (−155) was mutated in Constructs 2-Mt/G and 2-Mt/G&C. The CRE site (−26) was mutated in Constructs 3-Mt/C and 2-Mt/G&C. *Arrows* show the transcription initiation site reported by Kitagawa *et al.* (23). *Right*, luciferase activity of the vector constructs for the rat *PP2Acα* gene promoter in H9c2 cells. The cells were transiently transfected with the *PP2Acα* promoter-luciferase gene fusion plasmids. After 24 h of transfection, luciferase activity was assayed with cellular extracts as described under "Materials and Methods." Each value represents the mean of at least three independent experiments, and the S.D. was always within 10% of the mean.

Characterization of PP2Acα Gene Promoter—To investigate the mechanism of the transcriptional regulation of PP2Acα expression, we used the 1.6-kb genomic fragment containing the promoter region of PP2Acα inserted into a luciferase vector, pGL3 Basic. The transcriptional initiation site (nucleotide +1) was denoted in accordance with the report of Kitagawa *et al.* (23) (Fig. 6, *arrows*). The promoter region contains neither a TATA box nor a consensus CAAT sequence. The promoter region contains various transcription factor binding sites such as, CRE at position −26, GC box for Sp1 (31) at positions −155 and −10, and binding sites for receptor-related orphan receptor α (RORα) (32) at positions −778 and −553.

Both CRE and Sp1 Contribute to the Basal Expression of the PP2Acα Gene—In the report by Kitagawa *et al.* (23), a fragment of 118 bp (−162 to −44) was defined as the essential region for the gene expression of *PP2Acα*. As shown in Fig. 6, the deletion fragments of the gene promoter were made from the HindIII-digested fragment (−1209 to +258, full-length) (*Construct 1*), and subcloned into a pGL3 Basic vector. Then, the activity of luciferase was assayed with the cells transfected with each deletion mutant vector. The activity was fully maintained in the 537-bp fragment (−279 to +258) (*Construct 2*), but it decreased to ~65% of the full activity in the 403-bp fragment (−145 to +258) (*Construct 3*) containing the CRE site. In the upstream fragment of 1064-bp (−1209 to −145) (*Construct 6*) containing the GC box, the activity decreased to ~40% of the full activity. However, the activity was almost lost in the upstream fragment of 1044 bp (−1209 to −165) (*Construct 5*) and the downstream fragment of 259 bp (−1 to +258) (*Construct 4*). The results indicated that the full promoter activity was located in the sequence between −279 and −1. To examine whether the CRE and GC box contribute to the full promoter activity, disabled mutants were generated for the consensus sequences of CRE at −26 and GC box at −155 in the luciferase vector containing the 537-bp Construct 2. In Construct 2-Mt/G containing a CRE but no GC box, the activity decreased to ~70% of the full activity, and the level was similar to that of Construct 3. In Construct 2-Mt/G&C, the activity was significantly suppressed to less than 5% of full activity by both mutations. Furthermore, by the mutation with CRE, the activity was completely lost in Construct 3-Mt/C. Taken together, these results indicate that both the CRE and GC box contribute to the basal expression of the *PP2Acα* gene in H9c2 cells.

Thapsigargin Enhanced Protein-CRE Complex Formation—To examine if a DNA-binding protein like Sp1 or CREB could interact with the *PP2Acα* promoter, EMSA was performed with nuclear extracts from the cells treated with 5 μM thapsigargin or 10 μM BAPTA-AM using ^{32}P-labeled oligonucleotides designed for the GC box at −155 and CRE at −26. In the case of the CRE, a major band appeared but it disappeared in the presence of an excess of unlabeled probe (not shown) or ^{32}P-labeled probe with the disabled-mutant for CRE (Fig. 7, *A* and *C*). The intensity of shifted band for CRE significantly increased with the nuclear extracts treated with thapsigargin for 1–2 h (Fig. 7*A*, *left*). In contrast, the intensity decreased with the nuclear extracts treated with BAPTA-AM for 1–2 h (Fig. 7*A*, *right*). In the case of the GC box, a major band appeared but it too disappeared in the presence of an excess of unlabeled probe (not shown) or ^{32}P-labeled probe with the disabled mutant for GC box (Fig. 7, *B* and *C*). However, the band intensity was not influenced by the treatment with thapsigargin or BAPTA-AM (Fig. 7). In the case of the GC box-like site at −10, no major band was observed in EMSA, suggesting that the site is nonfunctional (data not shown). In the case of the RORα site at −553, a gel shift was observed but was not changed by the treatment with Ca^{2+} modulators such as thapsigargin and BAPTA-AM (data not shown). Furthermore, there was no gel-shift observed with the probe for the RORα site at −778 in EMSA, suggesting that the site is nonfunctional (data not shown). Together, these results indicate that the DNA

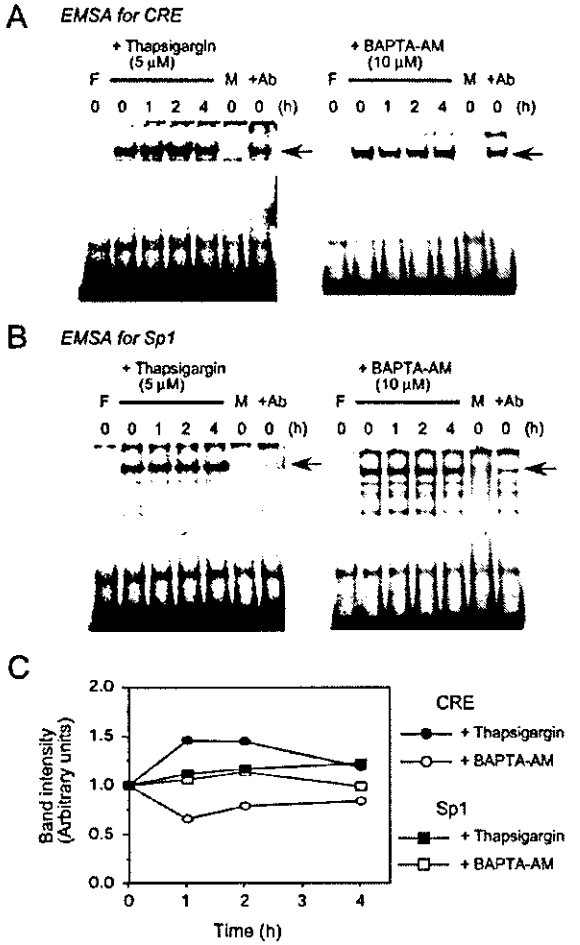

FIG. 7. **Ca^{2+} modulators influence DNA binding to CRE in EMSA.** H9c2 cells were incubated with thapsigargin (5 μM) or BAPTA-AM (10 μM) for the periods indicated, then the nuclear extracts were prepared as described under "Materials and Methods." ^{32}P-labeled oligonucleotides specific to CRE (−26) (*A*) and GC box (−155) (*B*) of the *PP2Acα* gene promoter were prepared and incubated with each nuclear extract, and then subjected to a 6% nondenatured PAGE. In *line F*, nuclear extract is free. In *line M*, ^{32}P-labeled mutant oligonucleotides were used for the original ones. In *line +Ab*, specific antibodies were added to the reaction mixture during the binding reaction for the supershift assay. *C*, quantitative data for the DNA binding to CRE and GC box shown in *A* and *B*. The intensity of gel-shift bands (*arrows*) was estimated densitometrically. Each value represents the mean of three experiments, and the S.D. was always within 10% of the mean.

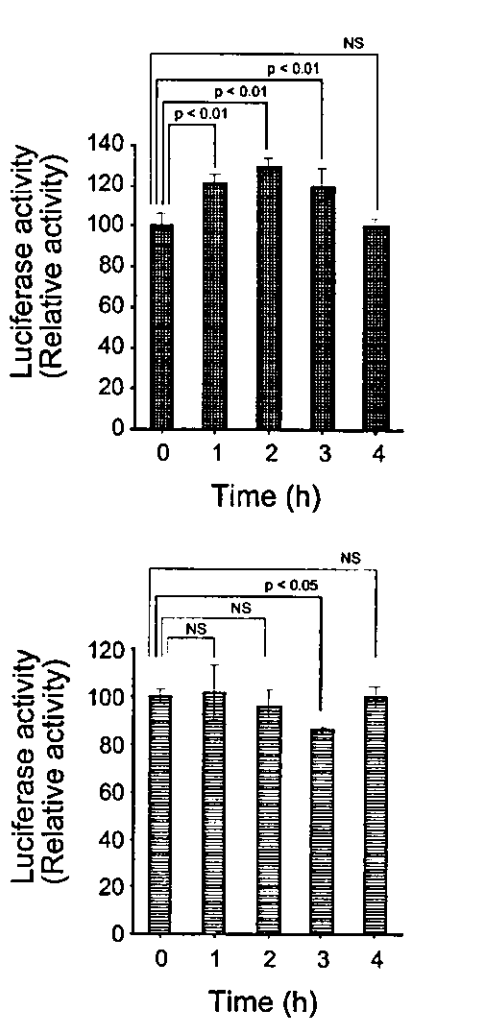

FIG. 8. **Ca^{2+} modulators influence the promoter activity of the rat *PP2Acα* gene in H9c2 cells.** H9c2 cells were transiently transfected with the *PP2Acα* promoter luciferase gene fusion plasmid (−145 to +258) (*Construct 3* in Fig. 6) containing CRE but no GC box. After 24 h of transfection, cells were treated with 5 μM thapsigargin (*A*) or 10 μM BAPTA-AM (*B*) for the periods indicated. Then luciferase activity was assayed with cell nuclear extracts as described under "Materials and Methods." Each value represents the mean ± S.D. of at least three experiments. The statistical analysis was performed with a factorial analysis of variance test.

binding activity involves both the CRE at −26 and GC box at −155, but it is specifically influenced by Ca^{2+} modulators, such as thapsigargin and BAPTA-AM, especially in the CRE at −26.

The Gene Promoter Activity of PP2Acα Is Regulated by Ca^{2+} Modulators via CRE—To confirm the CRE-dependent regulation of the gene expression of PP2Acα by Ca^{2+} modulators, the gene promoter activity was examined by assaying the luciferase activity as describe above. The cells were transfected with luciferase vector construct 3 (−145 to +258) (Fig. 6), which contains a CRE but no GC box. After 24 h of transfection, the cells were treated with 5 μM thapsigargin or 10 μM BAPTA-AM for predetermined periods, and the cell lysates were prepared and subjected to the assay for luciferase activity. As shown in Fig. 8*A*, the activity increased with thapsigargin to ~130% of the initial activity. The increase was not observed in the case of the disabled mutant for CRE with thapsigargin (data not shown). In contrast, with BAPTA-AM, the gene promoter activity decreased to ~85% of the initial level after 3 h of treatment, but returned to the initial level after 4 h (Fig. 8*B*). In the disabled mutant of CRE (*Construct 3-Mut/C* in Fig. 6), the promoter activity was lost and no activity was observed even on treatment with thapsigargin or BAPTA-AM (data not shown). Collectively, the results indicate that the gene expression of PP2Acα is transcriptionally regulated by the change of intracellular Ca^{2+} via CRE, and are consistent with the results of the EMSA for CREB binding (Fig. 6).

The Phosphorylation and Intracellular Localization of CREB Is Regulated by Ca^{2+} Modulators in H9c2 Cells—CREB is a pivotal transcription factor for the regulation of cellular survival, and its activation is mediated by phosphorylation at a specific residue, Ser-133 (33). To investigate the effect of Ca^{2+} modulators on the phosphorylation status of CREB, the level of CREB phosphorylated at Ser-133 was examined by immunoblot analysis using specific antibodies in the cells treated with thapsigargin or BAPTA-AM. As shown in Fig. 9*A*, the phosphorylation level of CREB increased on treatment with thapsigar-

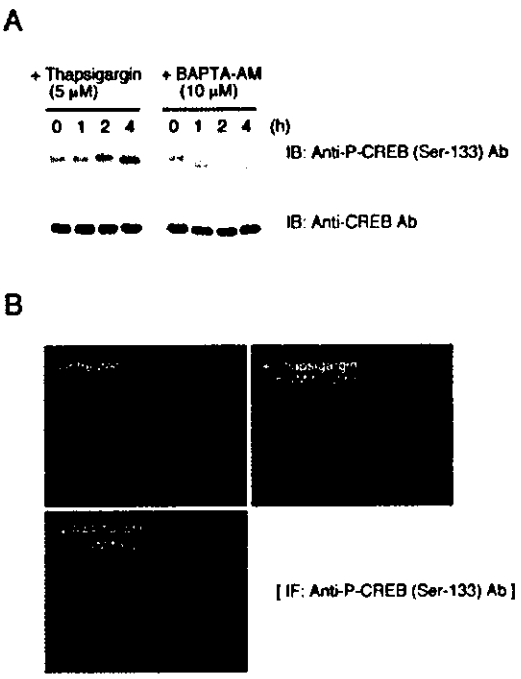

FIG. 9. **The phosphorylation of CREB is regulated by Ca^{2+} modulators in H9c2 cells.** *A*, H9c2 cells were incubated with thapsigargin (5 μM) or BAPTA-AM (10 μM) for the periods indicated, then cell extracts were prepared. The phosphorylation level of CREB was estimated by immunoblot analysis using specific antibodies. *B*, after the treatment with thapsigargin (5 μM) or BAPTA-AM (10 μM) for 2 h, the intracellular localization of phosphorylated CREB was examined by indirect immunofluorescence (*IF*) microscopy using specific antibodies as described under "Materials and Methods." The data represent two independent experiments.

gin, but decreased with BAPTA-AM, indicating that the phosphorylation status is regulated by the change of $[Ca^{2+}]_i$. In Fig. 9*B*, the intracellular localization of phosphorylated CREB (Ser-133) was investigated by indirect immunofluorescence microscopy in cells treated with or without the Ca^{2+} modulators. The fluorescent signals for phosphorylated CREB increased especially in the nucleus of the cells treated with thapsigargin, but it was significantly decreased by BAPTA-AM compared with untreated cells. These results are consistent with the results that the gene of *PP2Acα* is regulated via CRE in a Ca^{2+}-dependent manner.

DISCUSSION

Akt is a Ser/Thr protein kinase with antiapoptotic and oncogenic activities (8–10). With regard to the Ca^{2+}-dependent regulation of Akt, Conus *et al.* (15) reported that the activation of Akt was independent of Ca^{2+} in mouse fibroblasts treated with thapsigargin. However, Yano *et al.* (13) identified a Ca^{2+}-triggered signaling cascade in which CaMK kinase activates Akt in a PI 3-kinase-independent manner. Then Huber *et al.* (14) found that Akt was rapidly activated by treatment with thapsigargin through the activation of PI 3-kinase. In the present study, we found that Akt was suppressed by a long term elevation of $[Ca^{2+}]_i$ induced by thapsigargin, but was enhanced by a long term lowering of $[Ca^{2+}]_i$ caused by BAPTA-AM in H9c2 cells. The inactivation of Akt is highly correlated with susceptibility to apoptosis. Recently, Luo *et al.* (34) reported that inactivation of Akt is a causal mediator of cell death, and this is consistent with our present results. Although the underlying mechanism for these differences in the Ca^{2+}-dependent regulation of Akt was not clear, we showed that transcriptional regulation of PP2Acα was important to control the activation status of Akt in H9c2 cells under conditions where there is a long term change in $[Ca^{2+}]_i$ levels.

PP2A is a multifunctional protein Ser/Thr phosphatase that regulates a variety of signaling pathways in eukaryotic cells (35, 36, 37). The core structure is a dimer, consisting of a 36-kDa catalytic subunit (PP2Acα, β) and a 65-kDa constant regulatory (structural) subunit (PR65/Aα, β). A third, variable regulatory subunit (B, PR55/Bα, β, γ, δ; B′, PR56/61α, β, γ, δ, ϵ; B″, PR48/58/72/130; B‴, PR99/110) can associate with this core enzyme. There are various reports of PP2A as a positive regulator of apoptosis (38), although a specific subunit of PP2A containing B′/PR61 is reported to be inhibitory for apoptosis in *Drosophila* (39, 40). Bad is a pro-apoptotic member of the Bcl-2 family, whose function is highly regulated by reversible phosphorylation (41). PP2A was responsible for the dephosphorylation of Bad (42), and dephosphorylated Bad bound antiapoptotic Bcl-2 members at the mitochondrial membrane leading to apoptotic cell death (43). PP2A was also found to co-localize at the mitochondrial membrane with Bcl-2, and the proapoptotic sphingolipid ceramide has been shown to activate the PP2A involved (44, 45). In anti-Fas-induced apoptosis, activation of caspase-3 caused cleavage of the regulatory Aα subunit of PP2A, and this in turn increased PP2A activity (46). On the other hand, Liu *et al.* (47) reported that 4-hydroxynonenal induced dephosphorylation of Akt through activation of PP2A in a caspase-dependent apoptosis of Jurkat cells. In the study, the authors described that PP2A was activated by an altered intracellular localization of tyrosine-dephosphorylated PP2A, but not by the caspase-dependent cleavage of the regulatory Aα subunit of PP2A. Furthermore, C2-ceramide induced dephosphorylation of both GSK3β and Akt by activating PP2A, resulting in apoptosis in rat cerebellar granule cells, and the apoptosis was blocked with lithium by inhibiting PP2A activity (48). Together, these findings indicate that PP2A plays a critical role in the positive regulation of apoptosis by dephosphorylating various apoptotic regulators including Akt, but the molecular mechanism for the activation of PP2A in apoptosis is not clearly understood.

PP2A is considered a phosphatase responsible for the dephosphorylation and inactivation of Akt (47, 48, 49, 50, 51, 52, 53). Previously, we also showed that Akt was dephosphorylated by PP2A in H9c2 cells (16), and PP2A interacted transiently with Akt in H9c2 cells under oxidative stress with H_2O_2 (27). In the present study, the treatment with okadaic acid decreased PP2A activity to ~70% of the untreated control value, and it reversed the thapsigargin-dependent suppression of the phosphorylation of Akt in H9c2 cells (Fig. 4). Furthermore, treatment with okadaic acid could suppress the thapsigargin-induced enhancement of apoptosis in cells exposed to H_2O_2, although the effective okadaic acid concentration was limited to a range around 100–200 nM (Fig. 5). These findings strongly suggest that PP2A plays an up-regulating role in the thapsigargin-induced enhancement of apoptosis by inhibiting Akt signaling. Collectively, the finding that up-regulation of *PP2Acα* gene expression led to an increase of PP2A activity is consistent with the enhanced dephosphorylation and inactivation of Akt in H9c2 cells following the long term elevation of $[Ca^{2+}]_i$ due to thapsigargin exposure (Fig. 2). Although the expression of PP2Ac is tightly controlled by an autoregulatory translational mechanism (54), there are reports describing changes in PP2Ac levels, for instance, during all-*trans* retinoic acid-induced differentiation of HL-60 cells (55, 56), during adipocyte differentiation induced by peroxisome proliferator-activated receptor-γ (57), during stimulation by colony-stimulating factor in macrophages (58), and during a response to the disruption of cellular attachment in mouse C3 10T1/2 cells (59).

We also observed transcriptional activation of PP2Acα in H9c2 cells transfected with the expression vector for calreticulin, a molecular chaperone in the endoplasmic reticulum (16). However, the underlying mechanism for these differences in the regulation of PP2A expression was not clarified.

To investigate the molecular mechanism behind the Ca^{2+}-dependent transcriptional regulation of PP2Ac expression in H9c2 cells, the promoter function of the *PP2Acα* gene was characterized using a luciferase-based reporter assay in cells treated with Ca^{2+} modulators such as thapsigargin and BAPTA-AM. The results showed that the expression of PP2Acα was transcriptionally regulated by the change of $[Ca^{2+}]_i$. The *PP2Ac* gene has been isolated and characterized in humans (60) and rats (23). In both species, the promoter region of PP2Acα has a high GC content and does not contain either a TATA box or a CAAT box, which suggests that the gene is a typical housekeeping gene. Among various transcription factors including CREB, Sp1, and RORα within the promoter region, CREB was revealed to be responsible for Ca^{2+}-dependent regulation of the *PP2Acα* gene in H9c2 cells treated with thapsigargin and BAPTA-AM. CREB is a bZIP transcription factor that forms homo- or heterodimers with itself or other members of the CREB family including ATF1 and CREM, and is a pivotal transcription factor that regulates cell proliferation, differentiation, and survival in a variety of cell types in vertebrates (33). The CREB dimers interact with a specific DNA sequence having the consensus motif TGACGTCA in the regulatory region of CREB target genes. CREB is inactive as a transcription factor until a cell is exposed to any extracellular stimuli that trigger its phosphorylation at a specific site, Ser-133, within its kinase-inducible domain (33). CREB was originally identified as a target of the cAMP signaling pathway, and regulated in response to diverse signals, including peptide hormones, growth factors, and Ca^{2+}. CREB is known to be activated at high $[Ca^{2+}]_i$ and this is consistent with our findings that the level of CREB phosphorylated at Ser-133 increased with thapsigargin but decreased with BAPTA-AM in the nucleus of H9c2 cells. Though minute changes in $[Ca^{2+}]_i$ are quickly transformed into changes in the activity of several kinases including cAMP-dependent kinase, protein kinase C, MAPKs, Ca^{2+}/CaMK and CaMK kinase, it is not clear whether these kinases are influenced in the case of long term change of $[Ca^{2+}]_i$ in H9c2 cells treated with Ca^{2+} modulators. Among these kinases, CaMKII and CaMKIV were reported to be able to phosphorylate CREB directly (61, 62). In addition, Rsk protein kinase phosphorylates CREB at Ser-133 through activation of the Ras/MAPK signaling pathway by Ca^{2+} (63, 64). Although CaMKIV mediates the early phase in the phosphorylation of Ser-133 in membrane-depolarized neurons, the MAPK pathway is responsible for prolonging the phosphorylation (65). In the present study, an increase in both the phosphorylation of CREB at Ser-133 and activity of CREB to bind the CRE site was observed after 2 h treatment with thapsigargin, suggesting a late activation of CREB caused by the long term elevation of $[Ca^{2+}]_i$. The treatment with BAPTA-AM influenced the phosphorylation of CREB and suppressed the binding of CREB to the CRE after 1 h, and this also suggests a late inactivation of CREB on the long term suppression of $[Ca^{2+}]_i$. Taken together, the long term change of $[Ca^{2+}]_i$ may regulate CREB function through the MAPK pathway rather than CaMK pathway in H9c2 cells treated with Ca^{2+} modulators.

Thapsigargin causes an increase of $[Ca^{2+}]_i$, and is also known as an inducer of endoplasmic reticulum (ER) stress (unfolding protein stress in the ER) (66). Recently, Song *et al.* (67) reported that thapsigargin-induced ER stress induced dephosphorylation of both GSK3β and Akt by activating PP2A, resulting in apoptosis in neuroblastoma cells, and this was consistent with our results. In the study, the authors described that dephosphorylation of GSK3β by activated PP2A was critical for the activation of caspase-3 in ER stress-induced apoptosis, but the mechanism for the PP2A activation by ER stress was not clarified. In ER stress, a transcriptional up-regulation is seen in the ER stress responsive genes that code a variety of ER proteins related to molecular chaperone functions, such as BiP/Grp78, Grp94, Grp58/ERp57, ERp72, and calreticulin (66). In mammalian cells, the 19-nucleotide motif CCAAT-N9-CCACG was identified as an ER responsive element (ERSE) of various ER chaperone genes, and was recognized by the human bZIP transcriptional factor ATF6 for ER stress response (68). However, we could not find a consensus sequence within the 1.6-kbp promoter region of the *PP2Acα* gene, and this suggests that the *PP2Acα* gene is not a direct target for the ER stress response in thapsigargin-treated cells.

In this study, CREB was linked to the enhanced susceptibility to apoptosis through the induction of the *PP2Ac* gene in cells exposed to the long term elevation of $[Ca^{2+}]_i$. To further investigate whether CREB is specifically responsible for the up-regulation of apoptosis in cells treated with thapsigargin and H_2O_2, CREB expression was suppressed by the short interfering RNA (siRNA) for the CREB gene. Using mammalian CREB siRNA expression plasmid (pKD-CREB-v2, Upstate Biotechnology), the CREB expression level was suppressed in H9c2 cells to ~30% of non-transfected cells. Using the transfected cells, thapsigargin-dependent enhancement of cell damage and apoptosis were examined in cells treated with thapsigargin (5 μM) and H_2O_2 (75 μM). However, despite the suppression of CREB protein, cell damage and apoptosis were not inhibited in cells treated with thapsigargin and H_2O_2, but rather were more enhanced (data not shown). This indicates that CREB is not specifically responsible for the mechanism enhancing apoptosis in cells showing long term elevation of $[Ca^{2+}]_i$. However, this may be reasonable because CREB is well known as a transcription factor for cell survival and antiapoptotic genes such as Bcl-2 (69), and the suppression of CREB may firstly decrease the expression of such cell survival genes resulting in enhanced susceptibility to apoptosis. The effect of the suppressed expression of CREB on cell survival was also consistent with previous findings using dominant-negative CREB polypeptides (69). Although the suppressed expression of CREB itself did not specifically reduce the thapsigargin-dependent enhancement of apoptotic cell damage in H9c2 cells, it still may be possible that CREB works for apoptosis on some negative feedback-like loop of cell survival signaling in cells demonstrating long term elevation of $[Ca^{2+}]_i$.

In conclusion, we found that the Akt kinase pathway was regulated by a long term change of $[Ca^{2+}]_i$ through transcriptional regulation of PP2Acα. With an elevation of $[Ca^{2+}]_i$ induced by thapsigargin, *PP2Acα* gene expression is up-regulated through the activation of CRE at a late phase of the response. As a consequence, Akt is dephosphorylated and inactivated by PP2A, and this leads to an increase in susceptibility to apoptosis under the conditions with thapsigargin. Although the activation of CRE has been considered to function as a cell survival signaling, Ca^{2+}-induced late activation of CRE leads to an enhancement of apoptotic signaling, and this suggests some feedback mechanism of CRE-mediating cell survival signaling. Luo *et al.* (34) reported that NMDA-induced deactivation of Akt was causative of neural cell death, and this suggests some Ca^{2+}-dependent mechanism is involved in the inactivation of Akt. Although the Ca^{2+}-dependent regulation of cell survival and death has been extensively studied (1, 3, 4), the

present findings may indicate another novel regulatory pathway of Akt through PP2A in the cell survival signaling controlled by calcium homeostasis.

Acknowledgments—We thank Drs. Kunimi Kikuchi and Hiroshi Shima for generously providing the rat PP1αc and PP2Acα cDNAs, and useful suggestions. We also thank Midori Ikezaki and Akiko Emura for technical assistance.

REFERENCES

1. Berridge, M. J., Lipp, P., and Bootman, M. D. (2000) *Nat. Rev.* **1,** 11–21
2. Agell, N., Bachs, O., Rocamora, N., and Villalonga, P. (2002) *Cell. Signal.* **14,** 649–654
3. Orrenius, S., Zhivotovsky, B., and Nicotera, P. (2003) *Nat. Rev.* **5,** 552–565
4. Rizzuto, R., Pinton, P., Ferrari, D., Chami, M., Szabadkai, G., Magalhaes, P. J., Virgilio, F., and Pozzan, T. (2003) *Oncogene* **22,** 8619–8627
5. Murriel, C. L., and Mochly-Rosen, D. (2003) *Arch. Biochem. Biophys.* **420,** 246–254
6. Crabtree, G. R. (2001) *J. Biol. Chem.*, **276,** 2313–2316
7. Klumpp, S., and Krieglstein, J. (2002) *Curr. Opin. Pharmacol.* **2,** 458–462
8. Brazil, D. P., and Hemmings, B. A. (2001) *Trends Biochem. Sci.*, **26,** 657–664
9. Scheid, M. P., and Woodgett, J. R. (2003) *FEBS Lett.* **546,** 108–112
10. Franke, T. F., Hornik. C. P., Segev. L., Shostak. G. A., and Sugimoto. C. (2003) *Oncogene* **22,** 8983–8998
11. Ozes, O. N., Mayo, L. D., Gustin, J. A., Pfefer, S. R., Pfeffer, L. M., and Donner, D. B. (1999) *Nature* **401,** 82–85
12. Romashkova, J. A., and Makarov, S. S. (1999) *Nature,* **401,** 86–90
13. Yano, S., Tokumitsu, H., and Soderling, T. R. (1998) *Nature* **396,** 584–587
14. Huber, M., Hughes, M. R., and Krystal, G. (2000) *J. Immunol.* **165,** 124–133
15. Conus, N. M., Hemmings, B. A., and Pearson, R. B. (1998) *J. Biol. Chem.* **273,** 4776–4782
16. Kageyama, K., Ihara, Y., Goto, S., Urata, Y., Toda, G., Yano, K., and Kondo, T. (2002) *J. Biol. Chem.* **277,** 19255–19264
17. Hescheler, J., Meyer, R., Plant, S., Krautwurst, D., Rosenthal, W., and Schultz, G. (1991) *Circ. Res.* **69,** 1476–1486
18. Grynkiewcz, G., Poenie, M., and Tsien, R. Y. (1985) *J. Biol. Chem.* **260,** 3440–3450
19. Gavrieli, Y., Sherman, Y., and Benn-Sasson, S. A. (1992) *J. Cell Biol.* **119,** 493–501
20. Kitamura, K., Mizuno, Y., Sasaki, A., Yasui, A., Tsuiki, S., and Kikuchi, K. (1991) *J. Biochem.* **109,** 307–310
21. Kitagawa, Y., Tahira, T., Ikeda, I., Kikuchi, K., Tsuiki, S., Sugimura, T., and Nagao, M. (1988) *Biochim. Biophys. Acta.* **951,** 123–129
22. Ihara, Y., Sakamoto, Y., Mihara, M., Shimizu, K., and Taniguchi, N. (1997) *J. Biol. Chem.* **272,** 9629–9634
23. Kitagawa, Y., Shima, H., Sasaki, K., and Nagao, M. (1991) *Biochim. Biophys. Acta.* **1089,** 339–344
24. Muroya T., Ihara Y., Ikeda S., Yasuoka C., Miyahara Y., Urata Y., Kondo T., and Kohno S. (2003) *Biochem. Biophys. Res. Commun.* **309,** 905–910
25. Thastrup, O., Cullen, P. J., Drobak, B. K., Hanley, M. R., and Dawson, A. P. (1990) *Proc. Natl. Acad. Sci., U. S. A.* **87,** 2466–2470
26. Pan, Z., Bhat, M. B., Nieminen, A.-L., and Ma, J. (2001) *J. Biol. Chem.* **276,** 32257–32263
27. Murata, H., Ihara, Y., Nakamura, H., Yodoi, J., Sumikawa, K., and Kondo, T. (2003) *J. Biol. Chem.* **278,** 50226–50233
28. Dolmetsch, R. E., Lewis, R. S., Goodnow, C. C., and Healy, J. I. (1997) *Nature* **386,** 855–858
29. Haystead, T. A. J., Sim, A. T. R., Carling, D., Honnor, R. C., Tsukitani, Y., Cohen, P., and Hardie, D. G. (1989) *Nature* **337,** 78–81
30. Gehringer, M. M. (2004) *FEBS Lett.* **557,** 1–8
31. Bouwman, P., and Philipsen, S. (2002) *Mol. Cell. Endocrinol.* **195,** 27–38
32. Kane, C. D., and Means, A. R. (2000) *EMBO J.* **19,** 691–701
33. Shaywitz, A. J., and Greenberg, M. E. (1999) *Annu. Rev. Biochem.* **68,** 821–861
34. Luo, H. R., Hattori, H., Hossain, M. A., Hester, L., Huang, Y., Lee-Kwon, W., Donowitz, M., Nagata, E., and Snyder, S. H. (2003) *Proc. Natl. Acad. Sci., U. S. A.* **100,** 11712–11717
35. Milward, T. A., Zolnierowicz, S., and Hemmings, B. A. (1999) *Trends Biochem. Sci.* **24,** 186–191
36. Sontag, E. (2001) *Cell. Signal.* **13,** 7–16
37. Janssens, V., and Goris, J. (2000) *Biochem. J.* **353,** 417–439
38. Van Hoop, C., and Goris, J. (2003) *Biochim. Biophys. Acta* **1640,** 97–104
39. Silverstein, A. M., Barrow, C. A., Davis A. J., and Mumby M. C. (2002) *Proc. Natl. Acad. Sci., U. S. A.* **99,** 4221–4226
40. Li, X., Scuderi, A., Letsou, A., and Virshup, D. M. (2002) *Mol. Cell. Biol.* **22,** 3674–3684
41. Cory, S., Huang, D. C. S., and Adams, J. M. (2003) *Oncogene* **22,** 8590–8607
42. Chiang, C. W., Harris, G., Ellig, C., Masters, S. C., Subramanian, R., Shenolikar, S., Wadzinski, B. E., and Yang, E. (2001) *Blood* **97,** 1289–1297
43. Datta, S. R., Katsov, A., Hu, L., Petros, A., Fesik, S. W., Yaffe, M. B., and Greenberg, M. E. (2000) *Mol. Cell,* **6,** 41–51
44. Ruvolo, P. P., Deng, X., Ito, T., Carr, B. K., and May, W. S. (1999) *J. Biol. Chem.* **274,** 20296–20300
45. Ruvolo, P. P., Clark, W., Mumby, F., Gao, W. S., and May, W. S. (2002) *J. Biol. Chem.* **277,** 22847–22852
46. Santoro, M. F., Annand, R. R., Robertson, M. M., Peng, Y. W., Brady, M. J., Mankovich, J. A., Hackett, M. C., Ghayur, T., Walter, G. W., Wong, W. W., and Giegel, D. A. (1998) *J. Biol. Chem.* **273,** 13119–13128
47. Liu, W., Akhand, A. A., Takeda, K., Kawamoto, Y., Itoigawa, M., Kato, M., Suzuki, H., Ishikawa, N., and Nakashima, I. (2003) *Cell Death Differ.* **10,** 772–781
48. Mora, A., Sabio, G., Risco, A. M., Cuenda, A., Alonso J. C., Soler, G., and Centeno, F. (2002) *Cell. Signal.* **14,** 557–562
49. Andjelkovic, M., Jakubowicz, T., Cron, P., Ming, X.-F., Han, J.-W., and Hemmings, B.A. (1996) *Proc. Nat. Acad. Sci., U. S. A.* **93,** 5699–5704
50. Meier, R., Thelen, M., and Hemmings, B. A. (1998) *EMBO J.* **17,** 7294–7303
51. Chen, D., Ficini, R. V., Olson, A. L., Hemmings, B. A., and Pessin, J. E. (1999) *Mol. Cell. Biol.* **19,** 4684–4694
52. Resjo, S., Goransson, O., Harndahl, L., Zolnierowicz, S., Manganiello, V., and Degerman, E. (2002) *Cell. Signal.* **14,** 231–238
53. Ivaska, J., Nissinen, L., Immonen, N., Eriksson, J. E., Kahari, V. M., and Heino, J. (2002) *Mol. Cell. Biol.* **22,** 1352–1359
54. Baharian, Z., and Schonthal, A. H. (1998) *J. Biol. Chem.* **273,** 19019–19024
55. Tawara, I., Nishikawa, M., Morita, K., Kobayashi, K., Toyoda, H., Omay, S. B., Shima, H., Nagao, M., Kuno, T., Tanaka, C., and Shirakawa, S. (1993) *FEBS Lett.* **321,** 224–228
56. Nishikawa, M., Omay, S. B., Toyoda, H., Tawara, I., Shima, H., Nagao, M., Hemmings, B. A., Mumby, M. C., and Deguchi, K. (1994) *Cancer Res.* **54,** 4879–4884
57. Altiok, S., Xu, M., and Spiegelman, B. M. (1998) *Genes Dev.* **11,** 1987–1998
58. Wilson, N. J., Moss, S. T., Csar, X. F., Ward, A. C., and Hamilton, J. A. (1999) *Biochem. J.* **339,** 517–524
59. Campos, S. V., and Schonthal, A. H. (2000) *J. Cell. Physiol.* **182,** 88–96
60. Khew-Goodall, Y., Mayer, R. E., Maurer, F., Stone, S. R., and Hemmings, B. A. (1991) *Biochemistry* **30,** 89–97
61. Wu, X., and McMurray, C. T. (2001) *J. Biol. Chem.* **276,** 1735–1741
62. Kornhauser J. M., Cowan, C. W., Shaywitz, A. J., Dolmetsch, R. E., Griffith, E. C., Hu, L. S., Haddad, C., Xia, Z., and Greenberg, M. E. (2002) *Neuron* **34,** 221–233
63. Rosen, L., Ginty, D., Weber, M., and Greenberg, M. (1994) *Neuron* **12,** 1207–1221
64. Xing, J., Ginty, D. D., and Greenberg, M. E. (1996) *Science* **273,** 959–963
65. Wu, G.-Y., Deisseroth, K., and Tsien, R. W. (2001) *Proc. Natl. Acad. Sci., U. S. A.* **98,** 2808–2813
66. Kaufman, R. J. (1999) *Genes Dev.* **13,** 1211–1233
67. Song, L., De Sarno, P., and Jope, R. S. (2002) *J. Biol. Chem.* **277,** 44701–44708
68. Yoshida, H., Haze, K., Yanagai, H., Yura, T., and Mori, K. (1998) *J. Biol. Chem.* **273,** 33741–33749
69. Mayr, B., and Montminy, M. (2001) *Nat. Rev. Mol. Cell. Biol.* **2,** 599–609

Free Radical Biology & Medicine, Vol. 37, No. 11, pp. 1875–1884, 2004

0891-5849/$-see front matter

ELSEVIER

doi:10.1016/j.freeradbiomed.2004.09.002

Original Contribution

NUCLEAR GLUTATHIONE *S*-TRANSFERASE π PREVENTS APOPTOSIS BY REDUCING THE OXIDATIVE STRESS-INDUCED FORMATION OF EXOCYCLIC DNA PRODUCTS

KENSAKU KAMADA,*[,1] SHINJI GOTO,†[,1] TOMOHIRO OKUNAGA,* YOSHITO IHARA,†
KENTARO TSUJI,‡ YOSHICHIKA KAWAI,†[,2] KOJI UCHIDA,‡ TOSHIHIKO OSAWA,‡
TAKAYUKI MATSUO,* IZUMI NAGATA,* and TAKAHITO KONDO†

*Department of Neurosurgery and †Department of Biochemistry and Molecular Biology in Disease, Atomic Bomb Disease Institute, Nagasaki University Graduate School of Biomedical Sciences, Nagasaki 851-8523, Japan; and
‡Laboratory of Food and Biodynamics, Nagoya University Graduate School of Bioagricultural Sciences, Nagoya, Japan

(*Received* 7 *June* 2004; *Revised* 24 *August* 2004; *Accepted* 2 *September* 2004)
Available online 25 September 2004

Abstract—We previously found that nuclear glutathione *S*-transferase π (GSTπ) accumulates in cancer cells resistant to anticancer drugs, suggesting that it has a role in the acquisition of resistance to anticancer drugs. In the present study, the effect of oxidative stress on the nuclear translocation of GSTπ and its role in the protection of DNA from damage were investigated. In human colonic cancer HCT8 cells, the hydrogen peroxide (H_2O_2)-induced increase in nuclear condensation, the population of sub-G_1 peak, and the number of TUNEL-positive cells were observed in cells pretreated with edible mushroom lectin, an inhibitor of the nuclear transport of GSTπ. The DNA damage and the formation of lipid peroxide were dependent on the dose of H_2O_2 and the incubation time. Immunological analysis showed that H_2O_2 induced the nuclear accumulation of GSTπ but not of glutathione peroxidase. Formation of the 7-(2-oxo-hepyl)-substituted 1,N^2-etheno-2′-deoxyguanosine adduct by the reaction of 13-hydroperoxyoctadecadienoic acid (13-HPODE) with 2′-deoxyguanosine was inhibited by GSTπ in the presence of glutathione. The conjugation product of 4-oxo-2-nonenal, a lipid aldehyde of 13-HPODE, with GSH in the presence of GSTπ, was identified by LS/MS. These results suggested that nuclear GSTπ prevents H_2O_2-induced DNA damage by scavenging the formation of lipid-peroxide-modified DNA.

Keywords—Oxidative stress, DNA damage, Glutathione *S*-transferase π, 7-(2-Oxo-hepyl)-substituted 1,N^2-etheno-2′-deoxyguanosine adduct, Free radical

INTRODUCTION

The role of oxidative stress as a mediator of apoptosis has been extensively studied. In particular, hydrogen peroxide (H_2O_2), a by-product of oxidative stress and a major reactive oxygen species (ROS), has been implicated in triggering apoptosis in various cells. H_2O_2 induces peroxidation of cellular components such as proteins, lipids, and nucleic acids [1]. H_2O_2 also stimulates intracellular signal cascades, such as mitogen-activated protein kinases, and activates transcription factors, such as AP-1 and nuclear factor kappa-B [2].

Glutathione *S*-transferase (GST, EC 2.5.1.18) is mainly expressed in the cytoplasm and is ubiquitous in nature. GST functions in xenobiotic biotransformation [3], drug metabolism [4], protection against peroxidative stress of lipids and the nucleus [5–7], and isomeration of prostaglandins [8]. Human GSTπ is one of a family of

Address correspondence to: Takahito Kondo, Department of Biochemistry and Molecular Biology in Disease, Atomic Bomb Disease Institute, Nagasaki University Graduate School of Medicine, Nagasaki 851-8523, Japan; Fax: +81 (95) 849 7100; E-mail: kondo@net.nagasaki-u.ac.jp.

[1] Contributed equally to this work.

[2] Present address: Department of Food Science, Graduate School of Nutrition and Biosciences, University of Tokushima, Japan.

GSTs; it has been reported to accumulate in various human cancer tissues or precancer tissues and is employed in cancer research as a tumor marker [9–13]. An increase in GSTπ was also found in cancer cell lines resistant to doxorubicin hydrochloride (DOX), *cis*-diamminedichloroplatinum(II) (cisplatin: CDDP) [14–16], and alkylating agents [17].

In addition to its main location in the cytoplasm, GSTπ has been found in the nucleus in uterine cancer cells [18] and glioma cells [19]. These findings suggest a negative correlation between the existence of GSTπ in the nucleus of cancer cells and the survival of the patient. However, there has been no report on the mechanisms responsible for the nuclear survival of GSTπ or on the physiological role of nuclear GSTπ.

Edible mushroom lectin (*Agaricus bisporus* lectin; ABL) efficiently internalizes into the cytoplasm of cultured cells, localizes around the nucleus, and inhibits the nuclear transfer of proteins [20]. Previous reports presented evidence that ABL inhibits the nuclear transport of GSTπ and increases the sensitivity of cancer cells to anticancer drugs [21,22].

Endogenous lipid peroxidation products react with DNA and exocyclic DNA adducts to cause the covalent modification of nuclear bases [23,24]. During the lipid peroxidation process, lipid hydroperoxides are formed as the initial products, and the decomposition of the lipid hydroperoxides leads to the formation of aldehydes as the end products. Several aldehydes possess high reactivity against DNA bases, especially guanine [25–27]. Lipid-peroxide-induced DNA adduct formation and site-specific cleavage of double-stranded DNA have been reported [28,29]. Previously, Kawai et al. [30] studied the reaction of lipid hydroperoxides with DNA components and established a method to detect the formation of 7-(2 oxo-hepyl)-substituted 1,N^2-etheno-2′-deoxyguanosine adducts (oxo-heptyl-ϵdG) by the reaction of 13-hydroperoxyoctadecadienoic acid (13-HPODE) with 2′-deoxyguanosine (dG).

Recently, it was reported that 4-hydroxy-2-nonenal (4-HNE) and 4-oxo-2-nonenal (4-ONE), the end products of lipid peroxides, are nonenzymatically transformed to conjugate with GSH [31]. Moreover, 4-ONE, a major end product of 13-HPODE, had a higher affinity for the nucleus than 4-HNE. Even though it has been found that GSTs catalyzes the formation of a conjugate of 4-HNE with GSH [32], its role in the formation of 4-ONE-GSH adducts was not known. In this study, we examined whether the nuclear GSTπ plays a role in the cellular sensitivity to oxidative stress caused by H_2O_2 and found that GSTπ prevents DNA damage by scavenging the oxo-heptyl-ϵdG formed from 13-HPODE and forming a conjugate of 4-ONE with GSH.

MATERIALS AND METHODS

Materials

ABL was purchased from Wako Pure Chemical Industries Ltd. (Osaka, Japan). RPMI 1640 medium and fetal bovine serum (FBS) were obtained from Invitrogen Corp. (Carlsbad, CA). Sheep polyclonal antibodies against human glutathione peroxidase (GPX) were purchased from The Binding Site Ltd. (Birmingham, UK). Horseradish peroxidase (HRP)-labeled anti-rabbit IgG, HRP-labeled anti-mouse IgG, and HRP-labeled anti-sheep IgG were from DAKO A/S (Glostrup, Denmark). The Enhanced Chemiluminescence (ECL) kit was obtained from Amersham Biosciences (Buckinghamshire, UK). All other chemicals and reagents were purchased from Sigma Aldrich (St. Louis, MO).

Preparation of cells

We used the human cancer cell lines HCT8 (colonic carcinoma) kindly donated by Dr. K. J. Scanlon. HCT8 cells were supplemented with 10% FBS at 37°C in 5% CO2 with 100% humidity. Six hours before treatment with ABL, the cells were maintained in medium with 1% FBS. About 2×10^6 cells were harvested with trypsin and washed with phosphate-buffered saline (0.137 M NaCl, 2.68 mM KCl, and 10 mM NAH2PO4/Na2HPO4, pH 7.4: PBS) twice at 4°C. The pellets were stored at −80°C before use.

TUNEL assay

The terminal deoxynucleotidyl transferase-mediated dUTP nick end labeling (TUNEL) assay was performed using an Apop Tag Plus Fluorescein in situ Apoptosis Detection Kit (Intergen Co., Purchase, NY). Briefly, approximately 2×10^6 cells were harvested, fixed in 70% ethanol, treated with terminal deoxynucleotidyl transferase for 1 h and then flourescein isothiocyanate (FITC) conjugate anti-digoxigenin for 1 h at room temperature, washed with 0.1% Triton X-100/PBS, and resuspended in propidium iodide containing RNase A. Fluorescence intensity was estimated simultaneously using a FACScan flow cytometer (Becton–Dickinson, San Jose, CA).

Nuclear condensation

For the histochemical analysis, HCT8 cells were maintained with RPMI 1640 medium containing 10% FBS in a four-well Lab Tec Chamber (Nalge Nunc International, Naperville, IL). After treatment with H_2O_2, cells were treated with 10 μM Hoechst 33342 for 30 min to estimate the extent of nuclear condensation. They were then washed again with PBS. Fluorescence intensity was examined using an Axioskop2 fluorescence microscope (Carl Zeiss, Jena, Germany), and the findings were

analyzed using a charge-coupled device camera (Axio-Cam) and AxioVison software.

Analysis of double-stranded breaks of DNA

DNA damage was determined by flow cytometry, based on the formation of sub-G1 peaks of DNA as described by Gong et al. [33]. HCT8 cells were washed with PBS, fixed with 70% ethanol for 12 h at -20°C, and then centrifuged and further incubated with citrate–phosphate buffer (1 v of 0.1 M citric acid and 24 v of 0.2 M Na_2HPO_4) for 15 min at 25°C. The DNA content per nucleus was evaluated in a FACScan flow cytometer after the nuclei were stained with propidium iodide.

Preparation of proteins

The cytoplasmic and nuclear proteins were prepared as described by Digram et al. [34]. Proteins in the whole cells were prepared as described previously [35].

Preparation of antibodies

GSTπ was purified from human placenta, and polyclonal antibody against human GSTπ was obtained by immunizing rabbits as described previously [21]. The monoclonal antibody to Oxo-heptyl-edG was prepared as described previously [30].

Immunological estimation

Immunological levels of GSTπ in the cytoplasm and nucleus were estimated by Western blotting. Lysate from the extract of cells was separated by SDS–polyacrylamide gel electrophoresis (SDS–PAGE) in a 12.5% gel, transferred to a nitrocellulose membrane, and immunologically stained using rabbit IgG against human GSTπ or sheep IgG against human GPX as the primary antibody and HRP-labeled anti-rabbit IgG or HRP-labeled anti-sheep IgG as the secondary antibody. Blots were developed by enhanced chemiluminescence using the ECL kit and the relative immunological activity was analyzed by NIH Image. The protein concentration was determined according to Redinbaugh and Turley [36], with bovine serum albumin as the standard.

Estimation of lipid peroxide in the nucleus

Nuclei extracts were prepared as described by Abmayr and Warkman [37]. Nuclear thiobarbituric acid reactive substance (TBARS) levels were determined according to the method of Ohkawa et al. [38] using tetramethoxyprepane (Wako Pure Chemical Industries).

Estimation of oxo-heptyl-εdG

Cells incubated in various conditions were harvested with trypsin and washed with PBS two times at 4°C. The cells were then suspended in 10 mM citrate buffer (pH 6.0) and incubated for 10 min at 95°C. After a wash with PBS two times, the cells were suspended in 2 M HCl for 30 min at room temperature and rewashed with PBS two times. The levels of oxo-heptyl-εdG in the cells were estimated by flow cytometry using anti-oxo-heptyl-εdG mouse monoclonal antibody (mAb6A3) and FITC-conjugated anti-mouse IgG antibody.

Effect of GSTπ on the formation of oxo-heptyl-εdG

13-HPODE (20 mM) was mixed with 1 mM $FeCl_2$ and stood for 12 h at 37°C. The solution (13-HPODE, 5 mM and $FeCl_2$, 0.2 mM, as a final concentration) was incubated with or without GSH (1 or 5 mM) and GSTπ (0.2 U) in the presence of 5 μg of calf thymus DNA for 1 h at 37°C. Then 1 and 5 μg of DNA extracted from the solution by ethanol precipitation

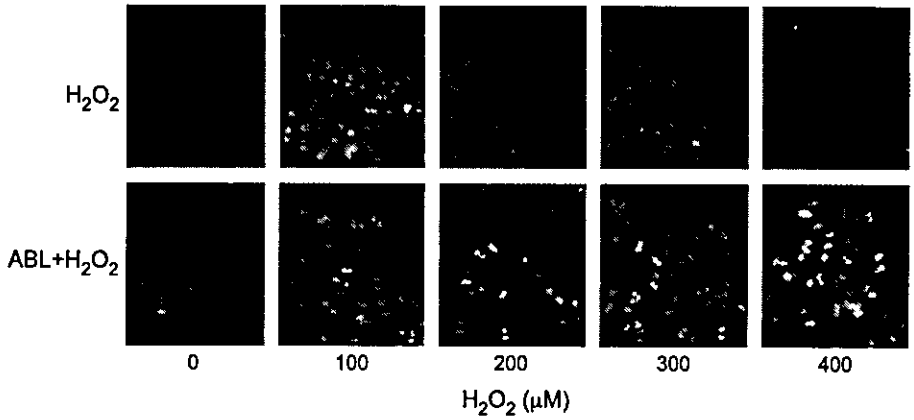

Fig. 1. Nuclear condensation. For the estimation of nuclear condensation, cells were incubated in a four-well Lab Tec Chamber. After treatment with various concentrations of H_2O_2 for 24 h, cells were treated with 10 μM Hoechst 33342 for 30 min for the estimation of nuclear condensation (top). The observation of fluorescence intensity was done using an Axioskop fluorescence microscope, and the findings were analyzed using a charge-coupled device camera and Axio Vision software. Cells were pretreated with ABL (40 μg/ml) for 10 h and then treated with H_2O_2 (bottom).

were spotted on a nitrocellulose membrane and immunologically stained using MAb6A3 as the primary antibody and HRP-conjugated anti-mouse IgG antibody as the secondary antibody. Blots were developed by enhanced chemiluminescence using the ECL kit and the relative immunological activity was analyzed by NIH Image.

Liquid chromatography/mass spectrometry

The chemical structure of the product of the incubation of 4-ONE and GSH in the presence of GSTπ was characterized by liquid chromatography/mass spectrometry (LC/MS). The LC/MS was conducted using a Platform II (VG Biotech) in an electrospray ionization positive (ESP+) mode. The gradient condition (solvent A, 0.01% trifluoroacetate; solvent B, acetonitrile containing 0.01% trifluoroacetate) was as follows: 100% A (0 min), 50% B (20 min), 100% B (30 min), 100% B hold (30–35 min), 100% A (40 min).

Statistical analysis

Data are presented as the mean ± SD. Differences were examined using a Student t test. A value of $p < 0.05$ was considered significant.

RESULTS

Nuclear condensation

Nuclear condensation is a characteristic of apoptosis. The nuclear condensation caused by H_2O_2 was estimated morphologically using Hoechst 33342 (Fig. 1). Human colonic cancer HCT8 cells were incubated with various concentrations of H_2O_2 for 24 h. No DNA condensation was observed (100–400 μM H_2O_2). ABL, a mushroom lectin, inhibits the nuclear transfer of GSTπ [1]. The cells were previously treated with 40 μg/ml of ABL for 10 h and further incubated with H_2O_2 for 24 h. Nuclear condensation was observed in

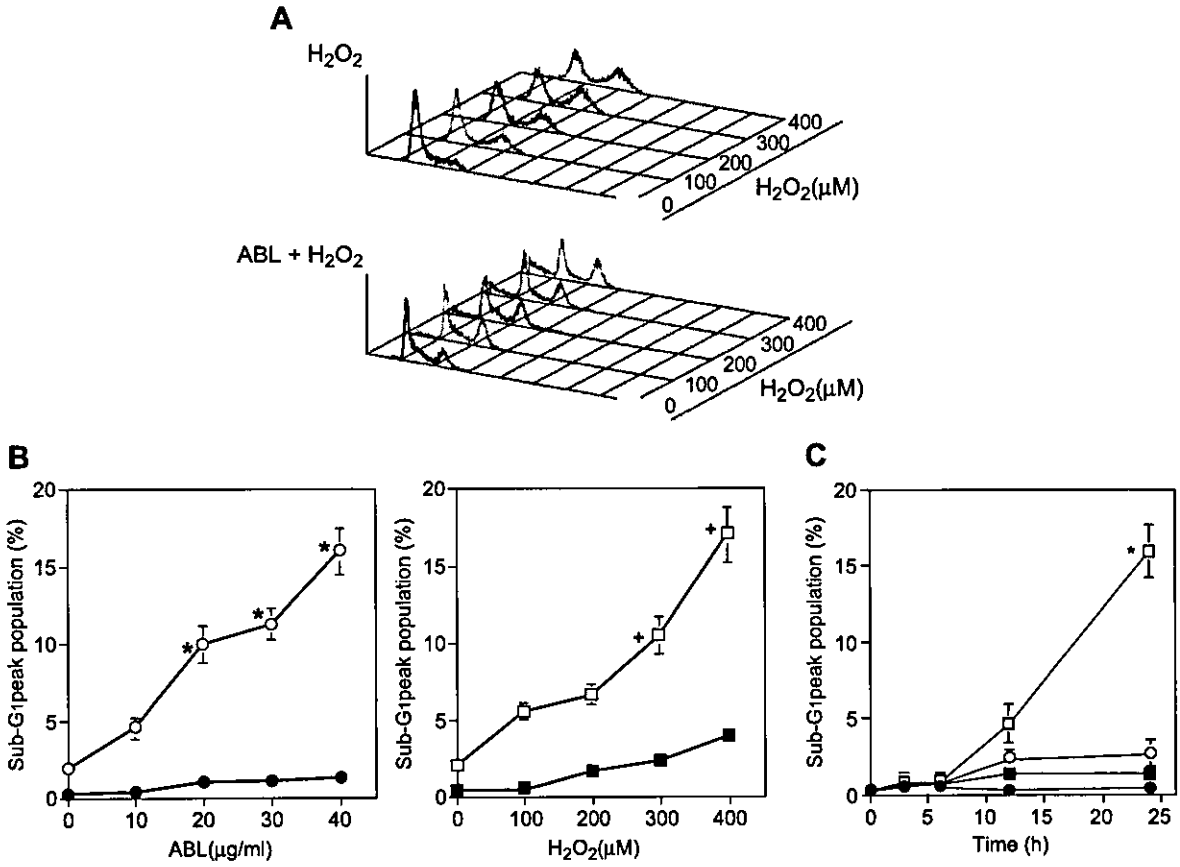

Fig. 2. Flow cytometric analysis of the DNA damage. (A) Effect of H_2O_2 on the DNA damage was analyzed using a FACScan flow cytometer. The sub-G_1 peak was estimated as a marker of the double-strand break of DNA. Treatment of cells with H_2O_2 or pretreatment with ABL was performed as described in Fig. 1 legend. (B) Effect of various concentrations of ABL (left) and H_2O_2 (right) on the formation of the sub-G_1 peak (%). ○400 μM H_2O_2 (+); ●H_2O_2 (−); □40 μg/ml ABL (+); ■ABL (−). *$p < 0.05$ compared with cells without H_2O_2 treatment. $^+p < 0.05$ compared with cells without ABL pretreatment. (C) Effect of incubation time on the formation of the sub-G_1 peak (%). ○400 μM H_2O_2 (+); ●control; □40 μg/ml ABL (+); □400 μM H_2O_2 with ABL pretreatment. *$p < 0.05$ compared with H_2O_2-treated cells. Data are the means of three independent analyses. Bars show the SD.

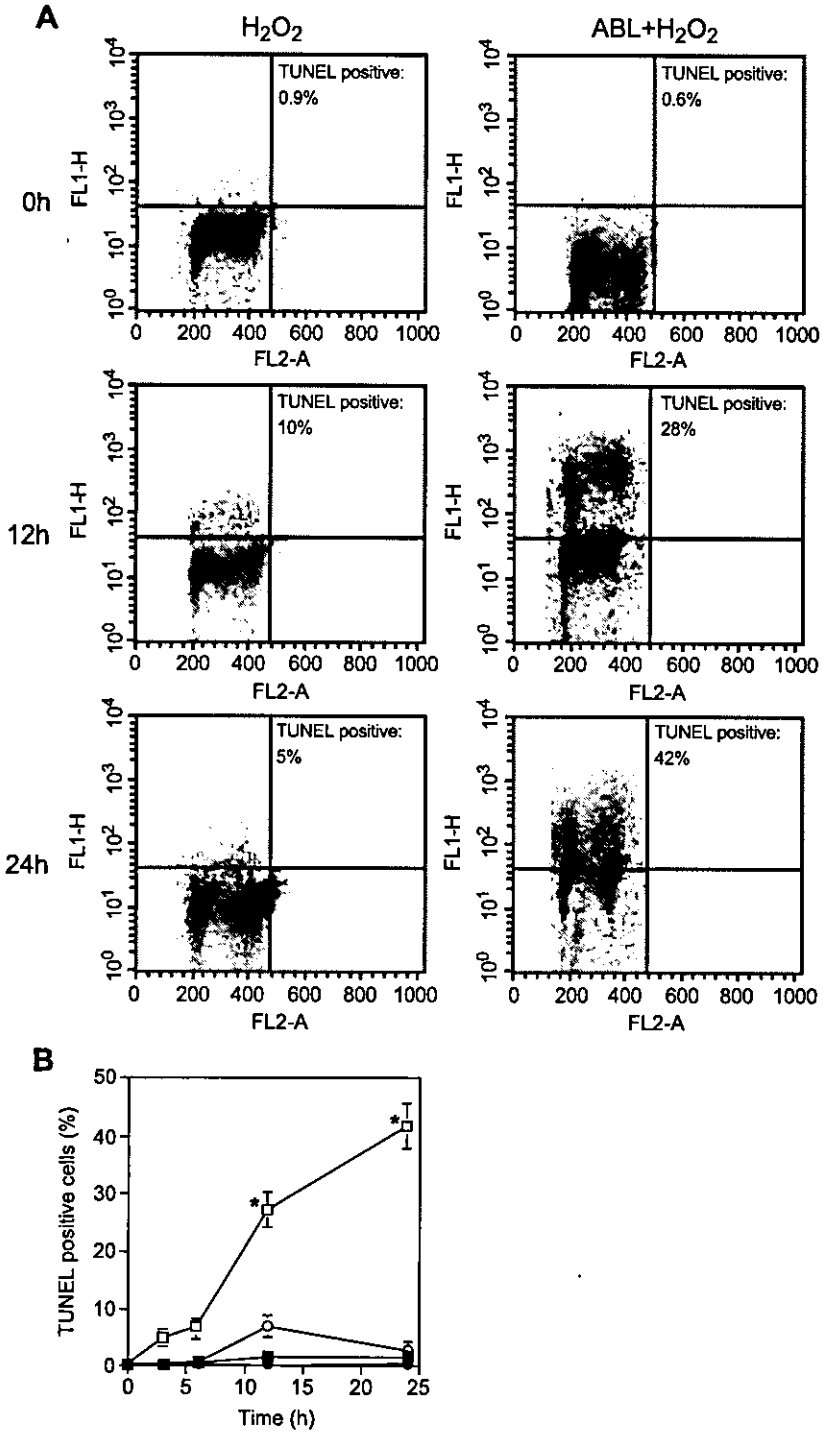

Fig. 3. TUNEL assay. The effect of ABL on the cytotoxicity of H_2O_2 was examined by TUNEL assay using an Apop Tag Plus Fluorencein In Situ Apoptosis Detection Kit as described under Materials and methods. (A) Cells (2×10^6) treated with 400 μM H_2O_2 for 12 and 24 h (left) or pretreated with ABL (40 μg/ml) for 10 h (right). (B) Effect of incubation time on the TUNEL-positive cells (%). O400 μM H_2O_2 (+); ●control; □40 μg/ml ABL (+); □400 μM H_2O_2 with ABL pretreatment. Data are the means of three independent analyses. Bars show the SD. *$p < 0.05$ compared with H_2O_2-treated cells.

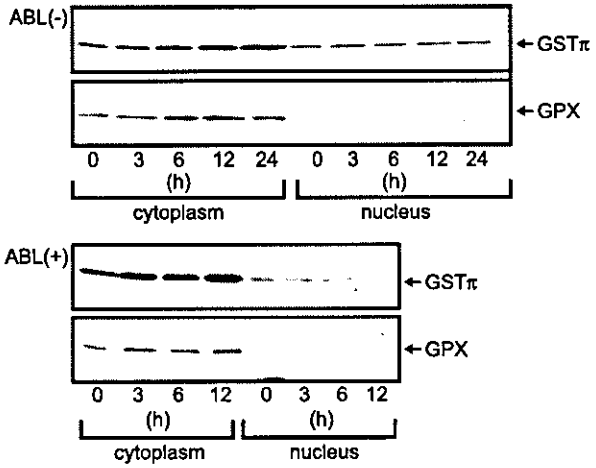

Fig. 4. Immunological estimation of the amount of GSTπ in the cytoplasm and nucleus. Proteins prepared from cellular cytoplasm and nucleus (1×10^5 cells) were separated by SDS–PAGE in a 12.5% gel, transferred to a nitrocellulose membrane, and immunologically stained using rabbit IgG or sheep IgG antibody against human GSTπ or GPX. Cells were treated with 400 μM H_2O_2 for the period indicated with (bottom) or without (top) pretreatment with ABL for 10 h.

a manner dependent on the dose of H_2O_2 when the cells were pretreated with ABL. These results suggest that inhibition of the nuclear transfer of GSTπ by ABL enhanced the H_2O_2-induced DNA damage.

Effect of H_2O_2 on DNA damage

To understand the extent of the DNA damage by H_2O_2, the sub-G_1 peak was estimated flow cytometrically as a marker of the double-stranded breaks of DNA (Fig. 2A). The DNA damage induced by pretreatment with ABL was not apparent (Fig. 2B, left) and damage was slightly induced by H_2O_2 alone (Fig. 2B, right). ABL increased the population of the sub-G_1 peak induced by 400 μM H_2O_2 in a dose-dependent (10–40 μg/ml) manner (Fig. 2B, left). Pretreatment with 40 μg/ml of ABL for 10 h enhanced the population of the sub-G_1 peak induced by H_2O_2 (100–400 μM) for 24 h dose dependently (Fig. 2B, right). The effect of ABL on the H_2O_2-induced DNA damage was dependent on the incubation time with H_2O_2 (Fig. 2C). These results suggest that ABL increases the sensitivity of cells to H_2O_2.

TUNEL assay

The H_2O_2-induced DNA damage was also estimated by TUNEL assay (Fig. 3). At 400 μM H_2O_2 increased the proportion of TUNEL-positive cells in 12 h (10%) with a subsequent decrease at 24 h (5%). Pretreatment with ABL (40 μg/ml) caused an increase in TUNEL-positive cells induced by 400 μM H_2O_2, 28% in 12 h and 42% in 24 h (Figs. 3A and 3B). These results also suggest that ABL increases the sensitivity of cells to H_2O_2, leading to DNA damage and apoptosis.

Immunological estimation of nuclear GSTπ

The amount of GSTπ induced by H_2O_2 was estimated. Fig. 4 shows results of Western blotting for GSTπ. H_2O_2 increased the levels of cytoplasmic GSTπ in a time-dependent manner (top). A concomitant increase in the level of GSTπ was observed in the nucleus. The effect of ABL on the nuclear transfer of GSTπ was studied (bottom). The H_2O_2-induced transfer of GSTπ to the nucleus was inhibited by ABL. The results were consistent with previous data [21].

In the cytoplasm, H_2O_2 is detoxified to H_2O by GPX. Then, the immunological activity of GPX was estimated (Fig. 4). Treatment with H_2O_2 increased the levels of GPX in the cytoplasm. During the experiment, no GPX was transferred to the nucleus. Similarly, the immunological activity of glutathione reductase was not found in the nucleus in the presence or absence of H_2O_2 (data not shown).

Estimation of lipid peroxide in the nucleus

The formation of lipid peroxides was determined as the TBARS levels (Fig. 5). H_2O_2 increased the levels of nuclear TBARS when the cells were pretreated with ABL.

Role of nuclear GSTπ

Kawai et al. [30] reported that DNA bases are modified with lipid peroxide of linoleic acids leading to DNA damage. 4-ONE is nonenzymatically formed from 13-HPODE, which reacts with dG to form oxo-heptyl-εdG. Doorn and Petersen [31] reported that 4-ONE has a higher affinity for nucleotides than 4-HNE and, on the other hand, spontaneously reacts with GSH to form its GSH conjugate [31]. We then speculated that

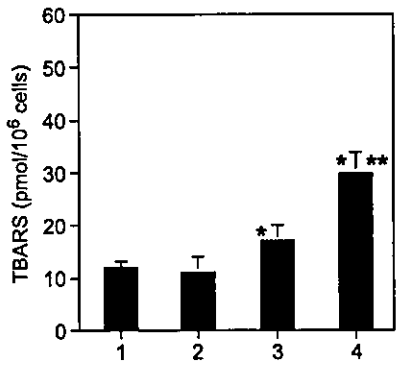

Fig. 5. Estimation of lipid peroxide in the nucleus. The formation of the nuclear TBARS was determined using tetramethoxyprepane. Data are the means of three independent analyses. Bars show the SD. $*p < 0.05$ compared with control cells. $**p < 0.05$ compared with H_2O_2-treated cells.

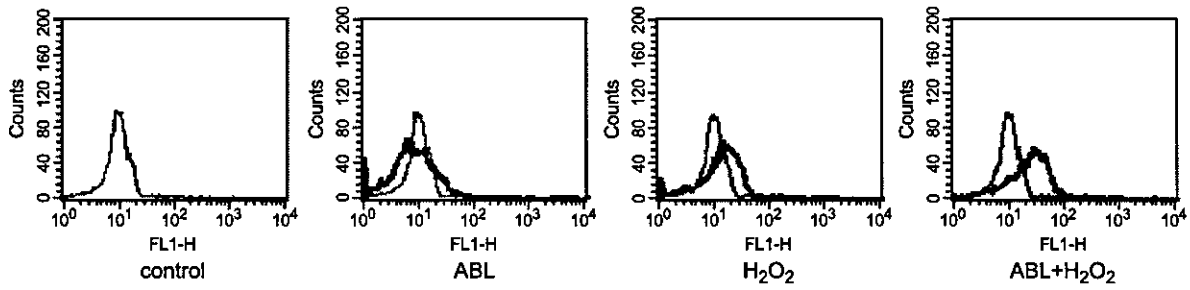

Fig. 6. Immunological estimation of oxo-heptyl-εdG. Effects of ABL (panel 2), H_2O_2 (panel 3), and H_2O_2 with ABL pretreatment (panel 4) on the levels of oxo-heptyl-εdG in the cells were estimated by flow cytometer using anti-oxo-heptyl-εdG mouse monoclonal antibody (mAb6A3) and FITC-conjugated anti-mouse IgG antibody.

human GSTπ catalyzed the formation of 4-ONE conjugated with GSH, which can then prevent the DNA from being modified with lipid peroxide. The immunological activity of lipid-peroxide-modified DNA was estimated flow cytometrically using anti-oxo-heptyl-εdG. The formation of oxo-heptyl-εdG was observed following treatment with 400 μM H_2O_2 for 12 h (Fig. 6, panel 3) and increased on pretreatment with ABL (Fig. 6, panel 4). The possible role of GSTπ in preventing the formation of lipid peroxide-DNA was affirmed in vitro. A mixture of 13-HPODE and $FeCl_2$ stood for 12 h at 37°C. The mixture was incubated with calf thymus DNA for 1 h at 37°C in the presence or absence of 5 mM GSH and 0.2 U of GSTπ. The formation of oxo-heptyl-εdG was estimated from immuno blots (Fig. 7). The formation of oxo-heptyl-εdG was inhibited by 20% in the presence of GSH (Fig. 7, lane 2) and by 60% in the presence of GSTπ and GSH (Fig. 7, lane 4). The results suggest that GSTπ inhibits the formation of oxo-heptyl-εdG in the nucleus. Fig. 8 shows the results of LC/MS measurements of the adduct formation of 4-ONE and GSH in the presence or absence of GSTπ. In the absence of GSTπ, the LC/MS analysis of the product gave a pseudomolecular ion peak [M + H]+ at *m/z* 462 (Fig. 8B). In the presence of GSTπ, this value apparently increased (Fig. 8C). Since the possible molecular weight of the ONE-GSH adduct is 641.18 (Fig. 9), the data obtained by LC/MS support the idea that GSTπ catalyzes the formation of the product.

DISCUSSION

In this study, we found for the first time that nuclear GSTπ functions to scavenge lipid-peroxide-induced DNA damage. We showed that (1) hydrogen peroxide increased the modification of nuclear DNA induced by lipid peroxide to cause DNA damage followed by the induction of apoptosis, (2) the nuclear GSTπ prevented DNA damage from lipid peroxide by scavenging the oxo-heptyl-εdG formed by the reaction of 13-HPODE with dG (the product of the conjugation of 4-ONE, one of the major breakdown products of 13-HPODE, with GSH catalyzed by GSTπ was identified), and (3) ABL inhibited the nuclear transfer of GSTπ to increase the sensitivity of the nucleus to oxidative stress. These findings suggest that nuclear GSTπ prevents H_2O_2-induced DNA damage by scavenging lipid-peroxide-modified DNA.

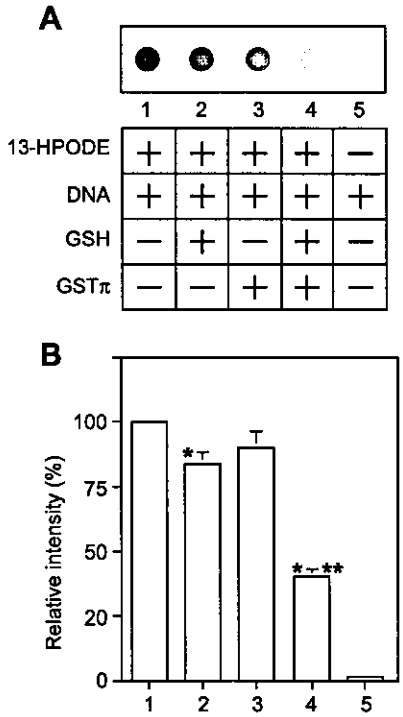

Fig. 7. Effect of GSTπ on the formation of oxo-heptyl-εdG in vitro. (A) 13-HPODE was mixed with $FeCl_2$ and stood for 12 h at 37°C. The solution was incubated with or without GSH and GSTπ in the presence of calf thymus DNA for 1 h at 37°C. DNA extract was spotted on a nitrocellulose membrane and immunologically stained using MAb6A3 as the primary antibody and HRP-conjugated anti-mouse IgG antibody as the secondary antibody. Blots were developed by enhanced chemiluminescence using the ECL kit and the relative immunological activity was analyzed by NIH Image. (B) Relative intensity (%) of the levels of oxo-heptyl-εdG in each lane corresponds to A. Data are the means of three independent analyses. Bars show the SD. $*p < 0.05$ compared with control cells; $**p < 0.05$ compared with H_2O_2-treated cells.

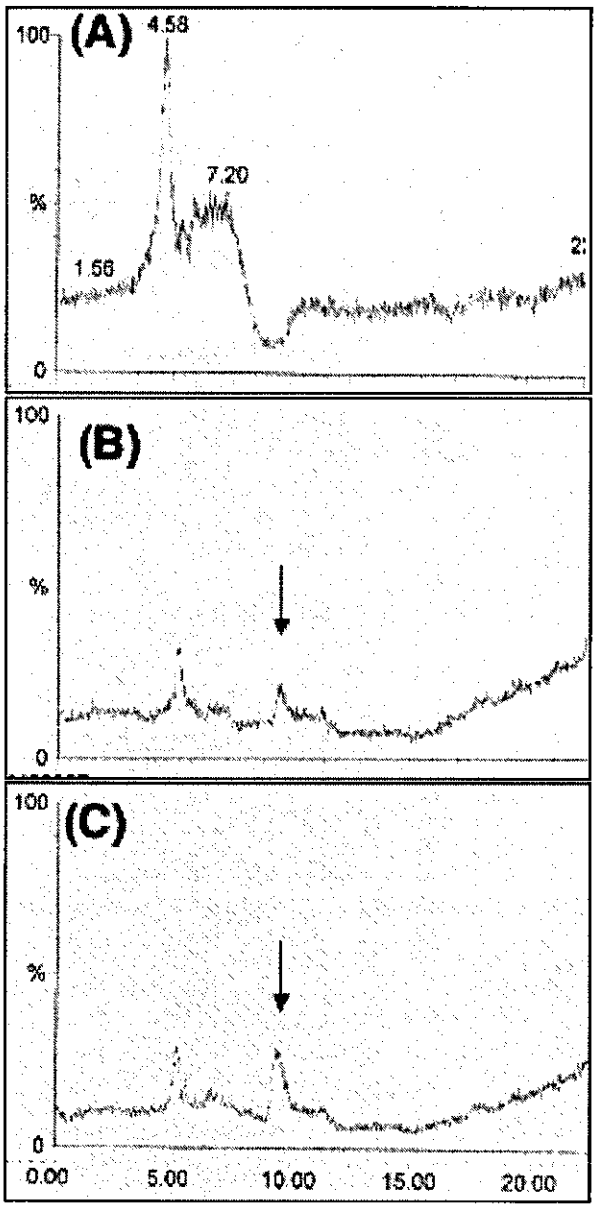

Fig. 8. LC/MS analysis. The chemical structure of the product of the incubation of 13-HPODE and GSH in the presence or absence of GSTπ was characterized by LC/MS. Materials were prepared as described in Fig. 6 legend. (A) 13-HPODE; (B) 13-HPODE with GSH; (C) 13-HPODE with GSH and GSTπ. Arrow indicates 4-ONE-GSH adduct.

Previously, we found that the nuclear GSTπ is an important factor in the acquisition of drug resistance in cancer cells [21,22]. Cancer cells which expressed the nuclear GSTπ in response to anticancer drugs such as DOX and CDDP showed resistance to these drugs, whereas the cells that did not express nuclear GSTπ were more sensitive to the drugs. The conjugation of the drugs with GSH was found in the resistant cells and correlated with decreased drug-induced DNA damage. In the present study, H_2O_2-induced DNA damage was observed when the cells were previously treated with ABL, an inhibitor of the nuclear transfer of GSTπ (Figs. 1–3). Strikingly, HCT8 cells were not sensitive to H_2O_2 (-400 μM). Treatment of the cells with H_2O_2 increased the nuclear transfer of GSTπ in a dose- (data not shown) and time-dependent manner (Fig. 4). The resistance of HCT8 cells to oxidative stress was abolished by pretreatment with ABL. The results strongly suggest an important role for the nuclear GSTπ in the sensitivity of the cells to oxidative stress.

There are many antioxidants in cells. Most of them are localized in the cytoplasm. In addition, each microorgan possesses its own defense system against oxidative stress. A nuclear superoxide dismutase, GPX, and GSTπ have been reported [21,39,40].

Adler et al. [41] reported that GSTp associates with Jun N-terminal kinase (JNK) to regulate its activity in mouse fibroblast NIH3T3 cells. Moreover, Yin et al. [42] demonstrated that GSTp coordinates the activation of extracellular signal-regulated kinases/p38 mitogen-activated protein kinase/inhibitor of κ kinase and suppression of JNK as part of the mechanism underlying its ability to elicit protection against H_2O_2-induced cell death. These findings indicate that GSTp plays an important role in the defense system against oxidative stress through its function as a regulator of stress kinases. It is interesting that GSTp has at least two different functions, to scavenge lipid peroxide and to regulate stress kinases as an antioxidant.

Lipid hydroperoxides are known to be relatively short lived. They are enzymatically and/or nonenzymatically metabolized to stable alcohols in vivo. They also react with metal to form reactive end products

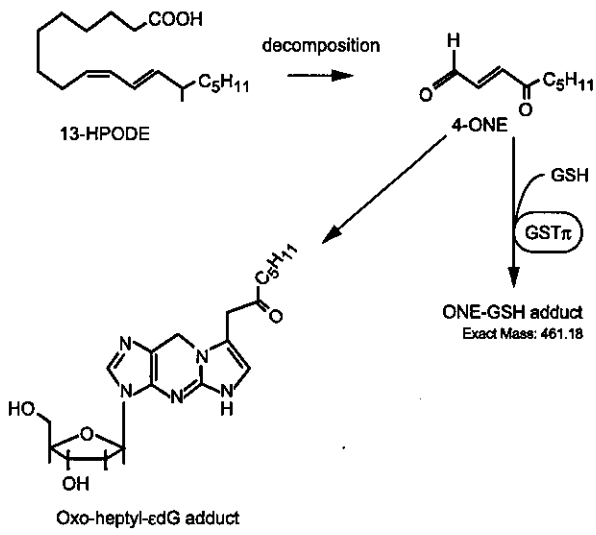

Fig. 9. Schema of the metabolism of 13-HPODE in the nucleus.

such as aldehydes. However, the importance of lipid hydroperoxides to the covalent modifications of biological components has not been thoroughly investigated. oxo-heptyl-εdG is formed by the reaction of 13-HPODE with dG [43]. During this reaction, 4-ONE directly mediates the formation of oxo-heptyl-εdG [30,43], suggesting that the lipid-hydroperoxide-derived production of 4-ONE contributes to DNA damage. 4-ONE and 4-HNE also form adducts with proteins. These adductions of proteins and DNA are thought to be involved in the pathogenesis of several diseases such as atherosclerosis [44], diabetes mellitus [45], and carcinogenesis [30].

With regard to the reduction of lipid peroxide, reduction of linoleic acid hydroperoxide by GPX was reported [46]. Lipid peroxide once formed is reduced to alcohol by GPX. With regard to the role of GST in the reduction of lipid peroxide, Cao et al. [32] reported that GSH and GST function in protecting against the cytotoxicity of 4-HNE in vascular smooth muscle cells. Depletion of GSH by buthionine sulfoximine and inhibition of GST activity by sufasalazine potentiated the 4-HNE-mediated cytotoxicity. The results suggested that GST functions to form a conjugate of 4-HNE with GSH.

Zimniak et al. [47] reported that mouse GSTA4-4 belongs to the alpha subclass of GST and functions to form a conjugate of 4-HNE with GSH. Additionally, Singhal et al. [48] reported that the human GST corresponding to mouse GSTA4-4 catalyzes the conjugation of 4-HNE with GSH. These reports indicate that GSTA4-4 plays an important role with GSH in the removal of 4-HNE. It is possible that GSTA4-4 functions to form a conjugate of 4-ONE with GSH. On the other hand, the colon cancer cell line employed in the present study possessed mainly GSTπ, which may detoxify 4-HNE and 4-ONE. It has been reported that aldose reductase prevents the formation of 4-HNE [49]. However, there has been no report on the role of GST in the reduction of another lipid peroxidation product, 4-ONE. As shown in Fig. 9, this is the first report to show that GSTπ reduces the formation of DNA adducts with 13-HPODE, characterized as oxo-heptyl-εdG. GSTπ catalyzes the conjugation of 4-ONE, a lipid-peroxide-derived product, with GSH, the adduct of which is thought to contribute to age-related diseases or carcinogenesis.

Acknowledgments—We are very grateful to Ms. Junko Takasaki for preparing the manuscript. This work was supported in part by Grants-in-Aid for Scientific Research from the Ministry of Education, Science, Sports, and Culture of Japan.

REFERENCES

[1] Kaneto, H.; Fujii, J.; Suzuki, K.; Kasai, H.; Kawamori, R.; Kamada, T.; Taniguchi, N. DNA cleavage induced by glycation of Cu,Zn-superoxide dismutase. *Biochem. J.* **304**:219–225; 1994.

[2] Nose, K.; Shibanuma, M.; Kikuchi, K.; Kageyama, H.; Sakiyama, T.; Kuroke, T. Transcriptional activation of early-response genes by hydrogen peroxide in a mouse osteoblastic cell line. *Eur. J. Biochem.* **201**:99–106; 1991.

[3] Jakoby, W. B. The glutathione S-transferases: a group of multifunctional detoxification proteins. *Adv. Enzymol. Relat. Areas Mol. Biol.* **46**:383–414; 1978.

[4] Chasseaud, L. F. The role of glutathione and glutathione S-transferases in the metabolism of chemical carcinogens and other electrophilic agents. *Adv. Cancer Res.* **29**:175–274; 1979.

[5] Prohaska, J. R.; Ganther, H. E. Glutathione peroxidase activity of glutathione-S-transferases purified from rat liver. *Biochem. Biophys. Res. Commun.* **76**:437–445; 1977.

[6] Meyer, D. J.; Beale, D.; Tan, K. H.; Coles, B.; Ketterer, B. Glutathione transferases in primary rat hepatomas: the isolation of a form with GSH peroxidase activity. *FEBS Lett.* **184**:139–143; 1985.

[7] Tan, K. H.; Meyer, D. J.; Coles, B.; Ketterer, B. Thymine hydroperoxide, a substrate for rat Se-dependent glutathione peroxidase and glutathione transferase isoenzymes. *FEBS Lett.* **207**:231–233; 1986.

[8] Ujihara, M.; Tsuchida, S.; Satoh, K.; Sato, K.; Urade, Y. Biochemical and immunological demonstration of prostaglandin D_2, E_2, and $F_{2\alpha}$ formation from prostaglandin H2 by various rat glutathione S-transferase isozymes. *Arch. Biochem. Biophys.* **264**:428–437; 1988.

[9] Satoh, K.; Kitahara, A.; Soma, Y.; Inaba, Y.; Hatayama, I.; Sato, K. Purification, induction, and distribution of placental glutathione transferase: a new marker enzyme for preneoplastic cells in the rat chemical hepatocarcinogenesis. *Proc. Natl. Acad. Sci. USA* **82**: 3964–3968; 1985.

[10] Kano, T.; Sakai, M.; Muramatsu, M. Structure and expression of a human class π glutathione S-transferase messenger RNA. *Cancer Res.* **47**:5626–5630; 1987.

[11] Mannervik, B.; Castro, V. M.; Danielson, U. H.; Tahir, M. K.; Hansson, J.; Ringborg, U. Expression of class Π glutathione transferase in human malignant melanoma cells. *Carcinogenesis* **8**:1929–1932; 1987.

[12] Howie, A. F.; Forrester, L. M.; Glancey, M. J.; Schlager, J. J.; Powis, G.; Beckett, G. J.; Hayes, J. D.; Wolf, C. R. Glutathione S-transferase and glutathione peroxidase expression in normal and tumour human tissues. *Carcinogenesis* **11**:451–458; 1990.

[13] Hirata, S.; Odajima, T.; Kohama, G.; Ishigaki, S.; Niitsu, Y. Significance of glutathione S-transferase-π as a tumor marker in patients with oral cancer. *Cancer* **70**:2381–2387; 1992.

[14] Saburi, Y.; Nakagawa, M.; Ono, M.; Sakai, M.; Muramatsu, M.; Kohno, K.; Kuwano, M. Increased expression of glutathione S-transferase gene in cis-diamminedichloroplatinum(II)-resistant variants of a Chinese hamster ovary cell line. *Cancer Res.* **49**: 7020–7025; 1989.

[15] Bai, F.; Nakanishi, Y.; Kawasaki, M.; Takayama, K.; Yatsunami, J.; Pei, X. H.; Tsuruta, N.; Wakamatsu, K.; Hara, N. Immunohistochemical expression of glutathione S-transferase-Π can predict chemotherapy response in patients with nonsmall cell lung carcinoma. *Cancer* **78**:416–421; 1996.

[16] Batist, G.; Tulpule, A.; Sinha, B. K.; Katki, A. G.; Myers, C. E.; Cowan, K. H. Overexpression of a novel anionic glutathione transferase in multidrug-resistant human breast cancer cells. *J. Biol. Chem.* **261**:15544–15549; 1986.

[17] Wang, Y. Y.; Teicher, B. A.; Shea, T. C.; Holden, S. A.; Rosbe, K. W.; al-Achi, A.; Henner, W. D. Cross-resistance and glutathione-S-transferase-π levels among four human melanoma cell lines selected for alkylating agent resistance. *Cancer Res.* **49**:6185–6192; 1989.

[18] Shiratori, Y.; Soma, Y.; Maruyama, H.; Sato, S.; Takano, A.; Sato, K. Immunohistochemical detection of the placental form of glutathione S-transferase in dysplastic and neoplastic human uterine cervix lesions. *Cancer Res.* **47**:6806–6809; 1987.

[19] Ali-Osman, F.; Brunner, J. M.; Kutluk, T. M.; Hess, K. Prognostic significance of glutathione S-transferase π expression and subcellular localization in human gliomas. *Clin. Cancer Res.* **3**:2253–2261; 1997.

[20] Yu, L. G.; Fernig, D. G.; White, M. R. H.; Spiller, D. G.; Appleton, P.; Evans, R. C.; Grierson, I.; Smith, J. A.; Davies, H.; Gerasimenko, O. V.; Petersen, O. H.; Milton, J. D.; Rhodes, J. M. Edible mushroom (*Agaricus bisporus*) lectin, which reversibly inhibits epithelial cell proliferation, blocks nuclear localization sequence-dependent nuclear protein import. *J. Biol. Chem.* **274**:4890–4899; 1999.

[21] Goto, S.; Ihara, Y.; Urata, Y.; Izumi, S.; Abe, K.; Koji, T.; Kondo, T. Doxorubicin-induced DNA intercalation and scavenging by nuclear glutathione S-transferase pi. *FASEB J.* **14**:2702–2714; 2001.

[22] Goto, S.; Kamada, K.; Soh, Y.; Ihara, Y.; Kondo, T. Significance of nuclear glutathione S-transferase pi in resistance to anti-cancer drugs. *Jpn. J. Cancer Res.* **9**:1047–1056; 2002.

[23] Burcham, P. C. Genotoxic lipid peroxidation products: their DNA damaging properties and role in formation of endogenous DNA adducts. *Mutagenesis* **13**:287–305; 1998.

[24] Marnett, L. J. Lipid peroxidation-DNA damage by malondialdehyde. *Mutat. Res.* **424**:83–95; 1999.

[25] Seto, H.; Okuda, T.; Takesue, T.; Ikemura, T. Reaction of malondialdehyde with nucleic acid. I. Formation of fluorescent pyrimido[1,2-a]purin-10 (3*H*)-one nucleosides. *Bull. Chem. Soc. Jpn.* **56**:1799–1802; 1983.

[26] Winter, C. K.; Segall, H. J.; Haddon, W. F. Formation of cyclic adducts of deoxyguanosine with the aldehydes *trans*-4-hyroxy-2-hexenal and trans-4-hydroxy-2-nonenal in vitro. *Cancer Res.* **46**: 5682–5686; 1986.

[27] Chung, F.-L.; Young, R.; Hecht, S. S. Formation of cyclic 1, N^2-propanodeoxyguanosine adducts in DNA upon reaction with acrolein or crotonaldehyde. *Cancer Res.* **44**:990–995; 1984.

[28] Wang, M.-Y.; Liehr, J. G. Lipid hydroperoxide-induced endogenous DNA adducts in hamsters: possible mechanism of lipid hydroperoxide-mediated carcinogenesis. *Arch. Biochem. Biophys.* **316**:38–46; 1995.

[29] Inouye, S. Site-specific cleavage of double-strand DNA by hydroperoxide of linoleic acid. *FEBS Lett.* **172**:231–234; 1984.

[30] Kawai, Y.; Kato, Y.; Nakae, D.; Kusuoka, O.; Konishi, Y.; Uchida, K.; Osawa, T. Immunohistochemical detection of a substituted 1,N^2-ethenodeoxyguanosine adduct by ω-6 polyunsaturated fatty acid hydroperoxides in the liver of rats fed a choline-deficient, L-amino acid-defined diet. *Carcinogenesis* **3**:485–489; 2002.

[31] Doorn J. A.; Petersen, D. R. Covalent adduction of nucleophilic amino acids by 4-hydroxynonenal and 4-oxononenal. *Chem. Biol. Interact.* **1**:143–144: 93–100; 2003.

[32] Cao, Z.; Hardej, D.; Trombetta, L. D.; Li, Y. The role of chemically induced glutathione and glutathione S-transferase in protecting against 4-hydroxy-2-nonenal-mediated cytotoxicity in vascular smooth muscle cells. *Cardiovasc. Toxicol.* **3**:165–177; 2003.

[33] Gong, J.; Traganos, F.; Darzynkiewicz, Z. A. Selective procedure for DNA extraction from apoptotic cells applicable for gel electrophoresis and flow cytometry. *Anal. Biochem.* **218**:314–319; 1994.

[34] Dignam, J. D.; Lebovitz, R. M.; Roeder, R. G. Accurate transcription initiation by RNA polymerase II in a soluble extract from isolated mammalian nuclei. *Nucleic Acids Res.* **11**:1475–1489; 1983.

[35] Goto, S.; Iida, T.; Cho, S.; Oka, M.; Kohno, S.; Kondo, T. Overexpression of glutathione S-transferase π enhances the adduct formation of cisplatin with glutathione in human cancer cells. *Free Radic. Res.* **31**:549–558; 1999.

[36] Redinbaugh, M. G.; Turley, R. B. Adaptation of the bicinchoninic acid protein assay for use with microtiter plates and sucrose gradient fractions. *Anal. Biochem.* **153**:267–271; 1986.

[37] Abmayr, S. M.; Warkman, J. L. *DNA-protein interactions*. In: Ausubel, F. M.; Brent, R.; Kingston, R. E.; Moore, D. D.; Seidman, J. G.; Smith, J. A.; Struhl, K., eds. Current protocols in molecular biology. Vol. 11. New York: Greene Publishing Asociates and Willey-Interscience. 1203–1219; 1987

[38] Ohkawa, H.; Ohishi, N.; Yagi, K. Assay for lipid peroxides in animal tissues by thiobarbituric acid reaction. *Anal. Biochem.* **95**:351–358; 1979.

[39] Ookawara, T.; Kizaki, T.; Takayama, E.; Imazeki, N.; Matsubara, O.; Ikeda, Y.; Suzuki, K.; Li Ji, L.; Tadakuma, T.; Taniguchi, N.; Ohno, H. Nuclear translocation of extracellular superoxide dismutase. *Biochem. Biophys. Res. Commun.* **296**:54–61; 2002.

[40] Nakamura, T.; Imai, H.; Tsunashima, N.; Nakagawa, Y. Molecular cloning and functional expression of nucleolar phospholipid hydroperoxide glutathione peroxidase in mammalian cells. *Biochem. Biophys. Res. Commun.* **311**:139–148; 2003.

[41] Adler, V.; Yin, Z.; Fuchs, S. Y.; Benezra, M.; Rosario, L.; Tew, K. D.; Pincus, M. R.; Sardana, M.; Henderson, C. J.; Wolf, C. R.; Davis, R. J.; Ronai, Z. Regulation of JNK signaling by GSTp. *EMBO J.* **18**:1321–1334; 1999.

[42] Yin, Z.; Vladimir, N. I.; Hasem, H.; Kenneth, T.; Ronai, Z. Glutathione S-transferase p elicits protection against H_2O_2-induced cell death via coordinated regulation of stress kinases. *Cancer Res.* **60**:4054–4057; 2000.

[43] Rindgen, D.; Nakajima, M.; Wehrli, S.; Xu, K.; Blair, I. A. Covalent modifications to 2′-deoxyguanosine by 4-oxo-2-nonenal, anovel product of lipid peroxidation. *Chem. Res. Toxicol.* **12**:1195–1204; 1999.

[44] Rosenfeld, M. E.; Palinski, W.; Yla-Herttuala, S.; Butler, S.; Witztum, J. L. Distribution of oxidation specific lipid-protein adducts and apolipoprotein B in atherosclerotic lesions of varying severity from WHHL rabbits. *Arteriosclerosis* **10**:336–349; 1990.

[45] Yamanouchi, J.; Takatori, A.; Itagaki, S.; Kawamura, S.; Yoshikawa, Y. APA hamster model for diabetic atherosclerosis. 2. Analysis of lipids and lipoproteins. *Exp. Anim.* **49**:267–274; 2000.

[46] Little, C.; O'Brien, P. J. An intracellular GSH-peroxidase with a lipid peroxide substrate. *Biochem. Biophys. Res. Commun.* **31**: 145–150; 1968.

[47] Zimniak, P.; Singhal, S. S.; Srivastava, S. K.; Awasthi, S.; Sharma, R.; Hyden, J. B.; Awasthi, Y. C. Estimation of genomic complexity, heterologous expression, and enzymatic characterization of mouse glutathione S-transferase mGSTA4-4 (GST5.7). *J. Biol. Chem.* **269**:992–1000; 1994.

[48] Singhal, S. S.; Zimniak, P.; Awasthi, S.; Piper, J. T.; He, N. G.; Teng, J. I.; Petersen, D. R.; Awasthi, Y. C. Several closely related glutathione S-transferase isozymes catalyzing conjugation of 4-hydroxynonenal are differentially expressed in human tissues. *Arch. Biochem. Biophys.* **311**:242–250; 1994.

[49] Vander Jagt, D. L.; Kolb, N. S.; Vander Jagt, T. J.; Chino, J.; Martinez, F. J.; Hunsaker, L. A.; Royer, R. E. Substrate specificity of human aldose reductase: identification of 4-hydroxynonenal as an endogenous substrate. *Biochim. Biophys. Acta* **1249**:117–126; 1995.

ABBREVIATIONS

ABL — edible mushroom (*Agaricus bispourus*) lectin
GPX — glutathione peroxidase
GSH — reduced form of glutathione
GST — glutathione *S*-transferase
LC/MS — liquid chromatography/mass spectrometry
Oxo-heptyl-εdG — 7-(2 oxo-hepyl)-substituted 1,N^2-etheno-2′-deoxyguanosine adduct
TBARS — thiobarbituric acid reactive substance
TUNEL — terminal deoxynucleotidyl transferase-mediated dUTP nick end labeling
4-HNE — 4-hydroxy-2-nonenal
4-ONE — 4-oxo-2-nonenal
13-HPODE — 13-hydroperoxyoctadecadienoic acid

PERGAMON

Journal of Steroid Biochemistry & Molecular Biology 85 (2003) 95–99

The Journal of Steroid Biochemistry & Molecular Biology

www.elsevier.com/locate/jsbmb

Androgen receptor functions from reverse genetic models☆

Takahiro Matsumoto[a,b], Ken-ichi Takeyama[a,b], Takashi Sato[a,b], Shigeaki Kato[a,b,*]

[a] *Laboratory of Nuclear Signaling, Institute of Molecular and Cellular Biosciences, University of Tokyo, 1-1-1 Yayoi, Bunkyo-ku, Tokyo 113-0032, Japan*
[b] *SORST, Japan Science and Technology, 4-1-8 Honcho, Kawaguchi, Saitama 332-0012, Japan*

Abstract

The androgen receptor (AR) is a ligand-dependent transcription factor involved in the regulation of many different physiological processes. AR dysfunction causes a diverse range of clinical conditions, including testicular feminization mutation (Tfm) syndrome, prostate cancer, and motor neuron disease (Kennedy's disease). However, due to lack of genetic models, the molecular basis of the AR in these disorders remains largely unknown. Using a conditional targeting technique based on the Cre-loxP system, we successfully generated null AR mutant (ARKO) mice. ARKO males exhibited normal healthy growth, but showed typical Tfm abnormalities. Hormonal assay of ARKO males revealed that while serum androgen levels were very low, estrogen levels were normal. Another hallmark of ARKO males was late-onset obesity, with marked accumulation of white adipose tissue. To clarify the role of human AR (hAR) mutants with expanded polyQ stretches as observed in neurodegenerative disease, we also established a *Dorsophila* model in which either wild-type or polyQ-expanded hAR were ectopically expressed. Although no overt phenotype was detected in adult fly-eye neurons expressing mutant hAR, the ingestion of androgen caused marked neurodegeneraton.

Keywords: Androgen receptor (AR); Androgen receptor knockout mouse (ARKO); Cre-loxP system; *Drosophila*-eye model; Kennedy's disease; PolyQ repeat; Testicular feminization mutation (Tfm)

1. Introduction

The androgen receptor (AR) plays an essential role in a variety of biological processes, not restricted to male reproductive functions such as Wolffian duct development and spermatogenesis [1,2]. Testosterone and its more potent metabolite, dihydrotestosterone, act as ligands for AR, and liganded AR activates the target gene expression at transcriptional level. Liganded AR form homodimers and bind specific DNA elements referred to as androgen responsive elements (*ARE*) in target gene promoters [3,4]. The *AR* gene comprises eight exons that encode a 110 kDa protein. Members of the steroid/thyroid hormone family share common structural features, with distinct functional domains referred to as domains A to E(F). The highly conserved middle region (C domain) acts as a DNA binding domain, while the ligand binding domain (LBD) is located in the C-terminal E/F domain. During ligand-induced transactivation, the N-terminal domains A/B and the steroid receptor LBD act as interacting regions for the co-activator complexes [5–7]. The autonomous activation function-1 (AF-1) within the A/B domain is ligand-independent, while AF-2 within the LBD is induced upon ligand binding [8]. While unliganded LBD appears to suppress the function of the A/B domain, ligand binding to the LBD is thought to evoke LDB function and restore A/B domain function through an, as yet undescribed, intramolecular alteration of the entire steroid receptor structure.

In contrast to the other members of the steroid receptor superfamily, a number of clinical disorders of the AR have been reported [9–14]. Classical AR functional abnormalities cause a spectrum of disorders of androgen insensitivity syndrome (AIS) or testicular feminization mutation (Tfm) [10,13,14]. AR mutations underlying these disorders include amino acid substitutions in the DNA or ligand binding domains, point mutations leading to premature stop codons, and deletions of the *AR* gene. In addition, expansion of a polyQ repeat region within AR has been implicated in the pathogenesis of a motor neuron disease called Kennedy's disease [9,12]. AR is a relatively large protein to other steroid receptors, due to the long N-terminal A/B domain that contains this polyQ repeat. However, the molecular basis of AR function underlying these AR-related disorders remains largely unknown due to the lack of stable genetic models. In this article, we present recent results of our studies into

☆ Presented at the 11th International Congress on Hormonal Steroids and Hormones and Cancer, ICHS & ICHC, Fukuoka, Japan, 21–25 October 2002.

* Corresponding author. Tel.: +81-3-5841-8478; fax: +81-3-5841-8477.
E-mail address: uskato@mail.ecc.u-tokyo.ac.jp (S. Kato).

0960-0760/$ – see front matter © 2003 Elsevier Science Ltd. All rights reserved.
doi:10.1016/S0960-0760(03)00231-0